Marine Micropaleontology
August 2020, Volume 150, Pages 101773 (35p.)
https://doi.org/10.1016/j.marmicro.2019.101773
https://archimer.ifremer.fr/doc/00512/62333/

A review of rare, poorly known, and morphologically problematic extant marine organic-walled dinoflagellate cyst taxa of the orders Gymnodiniales and Peridiniales from the Northern Hemisphere

Mertens Kenneth [1, *], Gu Haifeng [2], Gurdebeke Pieter R. [3], Takano Yoshihito [4], Clarke Dave [5], Aydin Hilal [6], Li Zhen [7], Pospelova Vera [7], Shin Hyeon Ho [8], Li Zhun [9], Matsuoka Kazumi [10], Head Martin J. [11]

[1] Ifremer, LER BO, Station de Biologie Marine, Place de la Croix, BP40537, F-29185 Concarneau CEDEX, France
[2] Third Institute of Oceanography, State Oceanic Administration, Xiamen 361005, China
[3] Department of Geology, Ghent University, Krijgslaan 281, S8, 9000 Ghent, Belgium
[4] Institute for East China Sea Research (ECSER), 1551-7 Taira-machi, Nagasaki 851-2213, Japan
[5] Shellfish Safety, Marine Institute, Oranmore, County Galway H91 R673, Ireland
[6] Faculty of Science and Arts, Department of Biology, Manisa Celal Bayar University, Şehit Prof. Dr. İlhan Varank Campus 45140, Yunusemre, Manisa, Turkey
[7] School of Earth and Ocean Sciences, University of Victoria, Bob Wright Centre A405, PO Box 1700, STN CSC, Victoria, BC V8W 2Y2, Canada
[8] Library of Marine Samples, Korea Institute of Ocean Science & Technology, Geoje 656-830, Republic of Korea
[9] Faculty of Marine Technology, Chonnam National University, Yeosu 59626, Republic of Korea
[10] Institute for East China Sea Research (ECSER), 1551-7 Taira-machi, Nagasaki 851-2213, Japan
[11] Department of Earth Sciences, Brock University, 1812 Sir Isaac Brock Way, St. Catharines, ON L2S 3A1, Canada

* Corresponding author : Kenneth Mertens, email address : kenneth.mertens@ifremer.fr

Abstract :

Dinoflagellates are a major component of the modern plankton. Of the 2192 species of marine free-living dinoflagellates presently described, an increasing number are being shown to produce resting cysts (probably hypnozygotes) within their life cycle. With rare exception, only the resting cysts fossilize, so they are of central importance in tracing the history of dinoflagellates through geological time. Cysts of many of the more common dinoflagellate species have distinctive morphologies allowing their geographic and stratigraphic occurrences to be traced. An ever-increasing number of taxa are also being shown to produce distinctive cysts, potentially increasing our knowledge of the diverse representation of dinoflagellates through time. Here the organic-walled cysts of 73 rare, poorly known or morphologically problematic marine dinoflagellate cyst species belonging to the orders Gymnodiniales (nine species) and Peridiniales (64 species) are reviewed, described and illustrated, and their stratigraphic ranges assessed. The names *Echinidinium aculeatum* and *Echinidinium transparantum* are validated herein.

Highlights

► 73 rare and endemic marine dinoflagellate cyst species are reviewed, described and illustrated. ► 9 belong to Gymnodiniales and 64 to Peridiniales. ► *Echinidinium aculeatum* and *Echinidinium transparantum* are validated.

Keywords : *Archaeperidinium, Diplopsalis, Dubridinium, Echinidinium, Gymnodinium, Lejeunecysta, Protoperidinium.*

Introduction

Dinoflagellates are a vital component of the modern plankton, comprising both autotrophic and heterotrophic species. Of the 2192 species of free-living marine dinoflagellates presently described (Gómez, 2012), an increasing number are being shown to produce resting cysts (probably hypnozygotes) within their life cycle. With rare exceptions, only the resting cysts have fossilization potential, so they provide a critical link to the history of dinoflagellates through geological time. Dinoflagellate cysts are now used commonly for the interpretation of past environments, ocean configurations, and climate evolution, and the demand for robust and precise reconstructions is increasing. Taxonomic detail and reliable identifications are crucial to the endeavour.

Modern dinoflagellate cysts and their biological affinities have been researched steadily since the 1960s (e.g., Wall and Dale, 1968; Bradford, 1975; Reid, 1977; Matsuoka, 1985). Of the dinoflagellate cyst species described and elucidated during this time (see Dale, 1983 and Matsuoka and Head, 2013 for a history of their study), some are rare and have yet to be decribed in detail and illustrated clearly. A useful and well illustrated atlas of dinoflagellate cysts was published by Rochon et al. in 1999, but this compilation dealt primarlily with northern North Atlantic taxa from which many rarer taxa, and especially many tropical and subtropical neritic species, were excluded. In addition, since 1999, many taxonomic advances have been made (e.g., Ellegaard and Moestrup, 1999; Head et al., 2001; Pospelova and Head, 2002; Liu et al., 2015a,b; Zonneveld and Pospelova, 2015; Gurdebeke et al., 2018). It has therefore become evident that an updated and more comprehensive compilation is needed.

The present compilation presents comparative descriptions and illustrations (Plate 1–19) for 73 rare or less well-known gymnodinialean and peridinialean species. Rare species are identified in fewer than than 40 sites in the database (de Vernal et al., this issue); the less well-known species have not yet been identified in the database. Although several species have an unknown response to palynological processing, their morphological similarity to species that do withstand palynological treatment suggests that they are similarly resistant and should appear in palynological preparations. In addition, round brown cysts with saphopylic archeopyles are illustrated in Figure 1, and species with theropylic archeopyles are illustrated in Figure 2. This review is restricted to marine organic-walled dinoflagellates; a comprehensive review of freshwater dinoflagellate cysts is given by Mertens et al. (2012a).

This contribution uses Kofoid labeling to describe plate tabulation, and dual nomenclature where available to link the separate taxonomies that have evolved for non-fossil and fossil dinoflagellates (Head et al., 2016).

Systematic part

Division DINOFLAGELLATA (Bütschli, 1885) Fensome et al., 1993
Class DINOPHYCEAE Pascher, 1914
Subclass GYMNODINIPHYCIDAE Fensome et al., 1993
Order GYMNODINIALES Apstein, 1909
Suborder GYMNODINIINEAE (Autonym)
Family GYMNODINIACEAE (Bergh, 1881a) Lankester, 1885

Genus *Barrufeta* Sampedro and Fraga in Sampedro et al., 2011
Comments. A motile-defined genus.

Cyst of *Barrufeta resplendens* (Hulburt, 1957) Gu et al., 2015a
Plate 1, figs. 1–6
Distinguishing characters. Ovoidal cysts with a pronounced cingulum. The living cyst has a prominent red body and is filled with granules. The cyst is covered by numerous hollow processes. The distal ends of processes form platforms with irregular margins. Adjacent processes may be connected proximally by crests, particularly in the cingular area. The cyst wall is light brown with a microgranular surface. The archeopyle is tremic with a zigzag margin and is located on the dorsal surface of the epicyst. Based on Gu et al. (2015a) and Mudie et al. (2017).
Dimensions. Central body 38.7–40.9 µm long and 35.2–36.0 µm wide, process length 5.2–5.8 µm (Gu et al., 2015a).
Remarks. The cysts do not survive palynological treatment according to Gu et al. (2015a), although Mudie et al. (2017) reported cysts following palynological treatment.
Biological affinity. *Barrufeta resplendens* according to Dale (1983, as *Gyrodinium resplendens*) and Gu et al. (2015a).

Stratigraphic range. Reported from Holocene sediments of the SE Black Sea (Mudie et al., 2017), and modern sediments of Georgian Sound (Wall et al., 1973), Chesapeake Bay (Dale, 1983) and the Gulf of Mexico (Gu et al., 2015a).

Genus *Gymnodinium* Stein, 1878
Comments. A motile-defined genus.

Cyst of *Gymnodinium catenatum* (Graham, 1942) Anderson et al., 1988
Plate 1, figs. 7–9
Distinguishing characters. A large red-brown cyst with a spherical body and a distinct microreticulate surface ornamentation. The ornamentation comprises numerous polygons reflecting the amphiesimal vesicles of the vegetative cells. Polygons vary in size (1–3 µm) and shape (3–8 sides). The living cyst is dark brown, contains many food reserves of starch and oil drops, and has a single red pigmented body. The laevorotatory cingulum is bordered by two parallel rows of oriented vesicles, with at least four rows of inner vesicles. The archeopyle is chasmic, but may follow a cingular margin for part of the rupture. Based on Anderson et al. (1988), Bolch et al. (1999) and Ribeiro et al. (2012a).
Dimensions. Cyst diameter 38–60 µm (Anderson et al., 1988), 36–62 µm (Bolch and Reynolds, 2002). Wall thickness is 0.6–1 µm (Anderson et al., 1988).
Remarks. Cysts of *Gymnodinium catenatum* can be distinguished from those of *Gymnodinium nolleri* and *Gymnodinium microreticulatum* by their larger size, although these can overlap. In addition, cysts of *Gymnodinium catenatum* have more than four inner rows of vesicles within the cingulum, whereas cysts of *Gymnodinium nolleri* have two or three such rows. Cysts of *Gymnodinium microreticulatum* have a similar number of rows as for the cysts of *Gymnodinium catenatum* but are smaller in size. The cingulum width relative to the cyst diameter is proportionally narrower on *Gymnodinium catenatum* cysts (<0.25 of the cyst diameter) than on either *Gymnodinium nolleri* or *Gymnodinium microreticulatum* (>0.25). Based on Bolch and Reynolds (2002) and Ribeiro et al. (2012a). The cysts withstand palynological treatment according to Anderson et al. (1988). The cyst wall does not show autofluorescence under ultraviolet excitation (Fukuyo et al., 2003, p. 106).
Biological affinity. *Gymnodinium catenatum* according to Anderson et al. (1988).
Stratigraphic range. Reported from Holocene sediments off the western Iberian shelf and estuaries (Amorim and Dale, 2006; Ribeiro et al., 2012a), including modern sediments from: Ria de Vigo, Spain (Anderson et al., 1988; García-Moreiras et al., 2018), off Australia and Tasmania (Sonneman and Hill, 1997; Bolch and Reynolds, 2002), the west coast of India (Godhe et al., 2000; D'Costa et al., 2008), the Gulf of California and the south-western Mexican coast (Morquecho and Lechuga-Deveze, 2003; Limoges et al., 2010), Japan (Matsuoka and Fukuyo, 1994), coastal waters of Korea (Pospelova and Kim, 2010),Yellow Sea of China (Gu et al., 2013), Aegean Sea (Aydin et al., 2011, as cyst of *Gymnodinium* cf. *nolleri*) and off Xiamen, East China Sea (this study).

Cyst of *Gymnodinium inusitatum* Gu et al., 2013
Plate 1, figs. 10–12
Distinguishing characters. A medium sized brown cyst with a distinct microreticulate surface ornamentation. The cysts are polygonal in outline, and display irregular folds of the wall. The archeopyle is chasmic. Living cysts contain large and irregular granules. Based on Gu et al. (2013).
Dimensions. Cyst length 48–51 µm, width 38–41 µm.
Remarks. This cyst differs from all other microreticulate cysts in its polygonal outline. It is not clear whether the cysts withstand palynological treatment.
Biological affinity. *Gymnodinium inusitatum* according to Gu et al. (2013).
Stratigraphic range. Reported from modern sediments from the Yellow Sea, China (Gu et al., 2013).

Cyst of *Gymnodinium microreticulatum* Bolch et al., 1999
Plate 2, figs. 1–3

Distinguishing characters. An unusually small pale brown spherical cyst with a distinct microreticulate surface ornamentation. The ornamentation comprises numerous polygons that vary in size and shape. At least three, usually four or five, rows of vesicles occur throughout the cingulum. Archeopyle chasmic, extends from the acrobase towards antapex, commonly oriented along the sulcus. Based on Bolch et al. (1999) and Bolch and Reynolds (2002).
Dimensions. Cyst diameter 17–28 µm (Bolch et al., 1999), 17–29 µm (Bolch and Reynolds, 2002), 23–35 µm (Amorim et al., 2002).
Remarks. Cysts of *Gymnodinium microreticulatum* are pale brown in contrast to the red-brown cysts of *Gymnodinium nolleri* (Bolch and Reynolds, 2002). In addition, cysts of *Gymnodinium nolleri* have proportionally larger vesicles in the cingulum, such that this area has only two to three rows of vesicles (Bolch and Reynolds, 2002). For further comparison with other microreticulate cysts, see remarks under cyst of *Gymnodinium catenatum*. The cysts withstand palynological treatment (e.g., Ribeiro et al., 2012a).
Biological affinity. *Gymnodinium microreticulatum* according to Bolch et al. (1999).
Stratigraphic range. Reported from Holocene sediments of the western Iberian shelf (Ribeiro et al., 2012a) including modern sediments off Australia and Tasmania (Bolch et al., 1999; Bolch and Reynolds, 2002), Daipeng Bay, China (Qi et al., 1996) and the Yellow Sea, China (Gu et al., 2013), the coast of Portugal (Amorim et al., 2002) and Prince Edward Island, eastern Canada (Price et al., 2016).

Cyst of *Gymnodinium nolleri* Ellegaard and Moestrup, 1999
Plate 2, figs. 4–6
Distinguishing characters. A small red-brown spherical cyst with a distinct microreticulate surface ornamentation. The ornamentation comprises numerous polygons that vary in size and shape. The cingulum and sulcus are expressed by rows of smaller vesicles. The archeopyle is chasmic and most often situated in the region of the cingulum. Two to four, usually three, uneven rows of vesicles (0.45–2.3 µm in maximum diameter) are present within the cingulum. Based on Ellegaard and Moestrup (1999).
Dimensions. Cyst diameter 28–38 µm (Ellegaard and Moestrup, 1999).
Remarks. For comparison with other microreticulate cysts, see remarks under cyst of *Gymnodinium catenatum*.
Biological affinity. The cysts were initially identified as belonging to *Gymnodinium catenatum* (e.g., Ellegaard et al., 1994) but later recognized as *Gymnodinium nolleri*, according to Ellegaard and Moestrup (1999). The cysts withstand palynological treatment (e.g., Ribeiro et al., 2012a).
Stratigraphic range. Reported from Holocene sediments of the western Iberian shelf (Ribeiro et al., 2012a; García-Moreiras et al., 2018) including modern sediments from coastal sites of the Skagerrak (Ellegaard et al., 1994, as *Gymnodinium catenatum*), and Kiel Bight and German North Sea (Nehring, 1994, 1995), and also sediment trap samples in the Cariaco Basin (Bringué et al., 2019).

Cyst of *Gymnodinium trapeziforme* Attaran-Fariman et al., 2007
Plate 2, figs. 7–9
Distinguishing characters. Trapezoidal to subrectangular pale brown to purple brown cysts that are dorsoventrally compressed with a distinct microreticulate surface ornamentation. The cingulum and sulcus are expressed by rows of smaller vesicles. Cingulum width approximately one quarter of the cyst length. Archeopyle chasmic, with variable orientation.
Dimensions. Cyst length 26–34 µm, width 20–27 µm, thickness 8–10 µm (Attaran-Fariman et al., 2007).
Remarks. This species is differentiated from all other microreticulate cysts by its atypical shape. The cysts withstand palynological treatment (K. Zonneveld, pers. comm. to KNM).
Biological affinity. *Gymnodinium trapeziforme* according to Attaran-Fariman et al. (2007).
Stratigraphic range. Reported from modern sediments of the southeast coast of Iran (Attaran-Fariman et al., 2007).

Genus *Margalefidinium* Gómez et al., 2017
Comments. A motile-defined genus.

Cyst of *Margalefidinium polykrikoides* (Margalef, 1961) Gómez et al., 2017 – East Asia ribotype
Plate 2, figs. 10–12
Distinguishing characters. Light brown, spherical cysts bearing connected processes. Living cysts have lipid bodies and a red accumulation body in the central part of the cell. The processes are connected by crests, forming irregular polygons. The wall is smooth and the archeopyle is unclear. Based on Li et al. (2015a).
Dimensions. Central body diameter 25.9–35.1 µm, process length ~3 µm (Li et al., 2015a).
Remarks. The cysts withstand palynological treatment as documented here. There is another cyst type that belongs to a different ribotype of the same species (Malaysia–American ribotype): this spherical brown cyst is illustrated in Tang and Gobler (2012) and needs restudy.
Biological affinity. *Margalefidinium polykrikoides* according to Li et al. (2015a, as *Cochlodinium polykrikoides*).
Stratigraphic range. Reported from modern sediments off Korea (Li et al., 2015a).

Family POLYKRIKACEAE Kofoid and Swezy, 1921

Genus *Polykrikos* Bütschli, 1873
Comments. A motile-defined genus.

Cyst of *Polykrikos hartmannii* Zimmermann, 1930
Plate 3, figs. 1–3
Distinguishing characters. Spinose round brown cysts that are light to medium brown bearing numerous hollow, striated, non-tabular, acuminate processes. Fine and discrete granules present on the central body. Archeopyle chasmic. Based on Matsuoka and Fukuyo, 1986).
Dimensions. Central body diameter 46–60 µm, process length 8–12 µm, length of archeopyle ca. 25 µm (Matsuoka and Fukuyo, 1986, p. 812).
Remarks. The cysts of *Polykrikos hartmannii* are somewhat similar to *Echinidinium granulatum*, but the latter has fewer processes which are relatively longer. In addition, the archeopyle is chasmic in *Polykrikos hartmannii* cysts but theropylic in *Echinidinium granulatum* (Head et al., 2001). The cysts withstand palynological treatment (Matsuoka and Fukuyo, 1986).
Biological affinity. *Pheopolykrikos hartmannii* (Zimmermann, 1930) Matsuoka and Fukuyo, 1986, according to Matsuoka and Fukuyo (1986); Hoppenrath et al. (2010) reattributed the species to *Polykrikos*.
Stratigraphic range. Reported from Upper Pleistocene sediments of the northern and western Pacific (Bujak and Matsuoka, 1986), Holocene sediments from the Black Sea and Marmara Sea (Mudie et al., 2017), India (Godhe et al., 2000) and the Santa Barbara Basin (Bringué et al., 2014), modern sediments off Japan (Matsuoka and Fukuyo, 1986), U.S.A. (Hoppenrath et al., 2010), Korea (Pospelova and Kim, 2010), Qingdao, Yellow Sea (this study), and from sediment trap samples of southern British Columbia (Pospelova et al., 2010; Price and Pospelova, 2011).

Cyst of *Polykrikos* sp.
Plate 3, figs. 4–6
Distinguishing characters. Light to dark brown cysts, ellipsoidal to sub-spherical in shape, with surface ornament comprising numerous processes consisting of irregular lobes. Cingulum and sulcus are not reflected. The archeopyle is chasmic. Based on Fukuyo (1982, as cyst of *Cochlodinium* sp.), Fukuyo et al. (2003, as *Cochlodinium polykrikoides* Margalef?), McMinn et al. (2010, as *Cochlodinium* sp.) and Mudie et al. (2017, as Cyst of *Cochlodinium* sensu Fukuyo 1982).
Dimensions. Cysts 60 to 80 µm long (Wall and Dale, 1968, as *Gyrodinium*? sp.), 25–45µm in diameter (Fukuyo et al., 2003), 25–33 µm long and 38–40 µm wide (McMinn et al., 2010).

Remarks. According to McMinn et al. (2010), the cyst is destroyed by palynological processing, although Verleye et al. (2009) and Mudie et al. (2017) reported specimens as withstanding palynological processing.
Biological affinity. According to McMinn et al. (2010), the cyst may be related to *Cochlodinium geminatum* (Schütt, 1895) Schütt, 1896; this needs confirmation. The latter species has been reclassified as *Polykrikos geminatum* (Schütt, 1896) Qiu et Lin in Qiu et al., 2013. Given the cyst morphology and the suggested relationship to *Polykrikos*, this species is here classified as cyst of an undetermined *Polykrikos* species.
Stratigraphic range. Reported from the Holocene of the Black Sea (Verleye et al., 2009), and modern sediments from Japan (Fukuyo, 1982), Arabian Sea (D'Silva et al., 2011), Pearl River estuary and Saanich Inlet (B.C., Canada) (this study).

Order PERIDINIALES Haeckel, 1894
Suborder PERIDINIINEAE (Autonym)
Family PROTOPERIDINIACEAE Balech, 1988
Subfamily DIPLOPSALIOIDEAE Abé, 1981
Comments. For several cysts of this subfamily it has not been established whether they withstand palynological treatment. However, similar cyst have been observed to survive such treatment but it is often not possible to unambiguously identify them to species level. These cysts are then commonly grouped as diplopsalid cysts (e.g., Mudie et al., 2017, plate-fig. 15, 1–6).

Genus *Boreadinium* Dodge and Hermes, 1981
Comments. A motile-defined genus.

Cyst of *Boreadinium breve* (Abé, 1981) Sournia, 1984
Plate 4, figs. 1–3
Distinguishing characters. Spherical to ovoidal cysts, pale brown in color, with a coarsely granular surface. The archeopyle is large and theropylic, possibly corresponding to plate 1a. Based on Liu et al. (2015a).
Dimensions. Cyst diameter 30–40 μm (Liu et al., 2015a).
Remarks. It is not clear whether the cysts withstand palynological treatment.

Biological affinity. *Boreadinium breve* according to Liu et al. (2015a).
Stratigraphic range. Modern sediments from the Yellow Sea, China (Liu et al., 2015a).

Genus *Diplopelta* Stein, 1883 ex Jörgensen, 1912
Comments. A motile-defined genus.

Cyst of *Diplopelta globula* (Abé, 1941) Balech, 1979
Plate 4, figs. 4–6
Distinguishing characters. The spherical cyst is dark brown with a smooth wall. The archeopyle is large and theropylic, apparently adnate along one margin (Plate 4, fig. 5), and corresponds to the plate 2a. Based on Liu et al. (2015a).
Dimensions. Cyst diameter 60 μm (Liu et al., 2015a).
Remarks. It is not clear whether the cysts withstand palynological treatment.

Biological affinity. *Diplopelta globula* according to Liu et al. (2015a).
Stratigraphic range. Modern sediments from the South China Sea (Liu et al., 2015a).

Cyst of *Diplopelta symmetrica* Pavillard, 1913
Plate 4, figs. 7–9

Distinguishing characters. Spherical cysts that are dark brown when cell contents are present, and light brown when empty. The moderately thick cyst wall is densely covered with hair-like processes. Cysts germinate through a zigzag theropylic archeopyle.
Dimensions. Central body diameter 37–50 µm, process length 1–4 µm (Dale et al., 1993).
Remarks. These cysts may not fossilize according to Dale et al. (1993), although they were observed by Verleye et al. (2009) following palynological treatment.
Biological affinity. *Diplopelta symmetrica* according to Dale et al. (1993).
Stratigraphic range. Holocene sediments from the Black Sea (Verleye et al., 2009) including modern sediments from Oslofjord, Norway and Fusaro Lagoon, Italy (Dale et al., 1993) and Bantry, Ireland (this study).

Genus *Diplopsalis* Bergh, 1881b emend. Liu et al., 2015a
Comments. A motile-defined genus.

Cyst of *Diplopsalis lenticula* Bergh, 1881b
Plate 4, figs. 10–12
Distinguishing characters. Cysts are smooth, spherical and pale brown to grey. The living cysts contain numerous pale droplets. The archeopyle is apical and theropylic, often V-shaped due to the inward rolling of the thin wall. This archeopyle was interpreted by Matsuoka (1988) as running along the apical boundary of the second precingular, first intercalary and fifth precingular plates. Based on Matsuoka (1988) and Lewis (1990).
Dimensions. Cyst body diameter 33–50 µm (Lewis, 1990).
Remarks. It is not clear whether the cysts withstand palynological treatment.

Biological affinity. *Diplopsalis lenticula* according to Matsuoka (1988), Lewis (1990) and Ellegaard et al. (1994).
Stratigraphic range. Modern sediments from Japan (Matsuoka, 1988), the U.K. (Lewis, 1990), Germany (Nehring, 1994), South China Sea, Yellow Sea (Liu et al., 2015a) and Denmark (Ellegaard et al., 1994).

Genus *Diplopsalopsis* Meunier, 1910
Comments. A motile-defined genus.

Cyst of *Diplopsalopsis latipeltata* Balech and Borgese, 1990
Plate 5, figs. 1–3
Distinguishing characters. Spherical cysts, dark brown when alive, with granular cell contents and without an accumulation body. Empty cysts are light brown. The cyst wall is smooth, and archeopyle theropylic probably representing the sutures between the single, wide intercalary plate and the cingular series. Based on Dale et al. (1993).
Dimensions. Cyst diameter 26–46.5 µm (Dale et al., 1993).
Remarks. These cysts may not fossilize according to Dale et al. (1993).
Biological affinity. *Diplopsalopsis latipeltata* according to Dale et al. (1993).
Stratigraphic range. Modern sediments from Fusaro Lagoon, Italy (Dale et al., 1993) and San Pedro Harbor, California (U.S.A.) (this study).

Cyst of *Diplopsalopsis ovata* (Abé, 1941) Dodge and Toriumi, 1993
Plate 5, figs. 4–6
Distinguishing characters. Spherical brown cysts with a smooth wall. The archeopyle is hexagonal and theropylic, corresponding to the 2a plate. Two flagellar scars are present. Based on Liu et al. (2015a).
Dimensions. Cyst diameter 40.0–50.0 µm (Liu et al., 2015a).

Remarks. It is not clear whether the cysts withstand palynological treatment. The cyst of a closely related species, *Diplopsalopsis orbicularis* (Paulsen, 1907) Meunier, 1910, as described by Wall and Dale (1968) and Matsuoka (1988), was equated with *Dubridinium cavatum* Reid, 1977 by Dale (1983).
Biological affinity. *Diplopsalopsis ovata* according to Liu et al. (2015a).
Stratigraphic range. Modern sediments from the Yellow Sea, China (Liu et al., 2015a) and Sasebo, Japan (this study).

Genus *Dubridinium* Reid, 1977
Comments. A cyst-defined genus.

Dubridinium caperatum Reid, 1977
Plate 5, figs. 7–9
Distinguishing characters. Dark brown oblate cysts with slight dorsoventral compression, and circular to sub-circular in polar view. Two layers: a thick microgranular inner layer and a thin smooth outer layer, which displays cingulum, as raised folds, and sulcus. Archeopyle theropylic, following cingulum, operculum adnate ventrally. Based on Reid (1977), Matsuoka (1988), and Sonneman and Hill (1997).
Dimensions. Cyst minimum diameter 40–51 µm, maximum diameter 42–56 µm (Reid, 1977).
Remarks. This species of *Dubridinium* differs from other species in its thick walled microgranular inner wall and its closely attached outer layer (Reid, 1977). The cysts withstand palynological treatment (Reid, 1977).
Biological affinity. *Preperidinium meunieri* (Pavillard, 1913) Elbrächter, 1993, according to Reid (1977, as *Diplopeltopsis minor*) and Matsuoka (1988, as *Zygabikodinium lenticulatum*).
Stratigraphic range. Holocene including modern sediments from the Black Sea (Mudie et al., 2017) and modern sediments from the U.K. (Reid, 1977), Korea (Cho et al., 2003; Shin et al., 2007, 2010a, 2010b; Pospelova and Kim, 2010), Izmir Bay (Aydin et al., 2010), Tasmania and South Australia (McMinn et al., 2010) and around Vancouver Island (Krepakevich and Pospelova, 2010).

Dubridinium cassiculum Reid, 1977
Plate 5, figs. 10–12
Distinguishing characters. Cavate circular to sub-circular cysts in polar view, usually with polar compression. Central body thick walled, smooth, covered by a closely attached outer layer which is folded into a reticulum with laminae 2 µm wide giving the surface a fenestrate appearance. Folds in the outer layer outline the cingulum and sulcus. Discrete granules may also delineate the cingulum. Based on Reid (1977).
Dimensions. Central body minimum diameter 24–34 µm, maximum diameter 35–47 µm (Reid, 1977).
Remarks. *Dubridinium cassiculum* differs from other *Dubridinium* speces in the smooth, thick walled nature of the inner layer and the reticulations of the outer layer (Reid, 1977). The cysts withstand palynological treatment (Reid, 1977).
Biological affinity. Unknown.
Stratigraphic range. Modern sediments from the U.K. (Reid, 1977).

Dubridinium cavatum Reid, 1977
Plate 6, figs. 1–3
Distinguishing characters. Spherical or ovoid cysts. Central body thin with a scabrate or finely microgranular surface. Outer layer membranous, may be close or distant from inner layer, and may reflect the position of the cingulum by forming two parallel folds. Between wall layers, granular inclusions are found which appear to act as supports for the outer layer. Archeopyle theropylic, following anterior margin of cingulum, operculum adnate in mid-ventral area. Based on Reid (1977).
Dimensions. Central body minimum diameter 35–58 µm, maximum diameter 42–58 µm (Reid, 1977).

Remarks. The size, ornament of the inner layer and granules between the two wall layers distinguish this species from *Dubridinium caperatum*, *Dubridinium cassiculum*, and *Dubridinium ulsterum* (Reid, 1977). The cysts withstand palynological treatment (Reid, 1977).
Biological affinity. Equated with *Diplopsalopsis orbicularis* (Paulsen, 1907) Meunier, 1910, by Reid (1977) and Dale (1983).
Stratigraphic range. Modern sediments from the U.K. (Reid, 1977).

Dubridinium ulsterum Reid, 1977
Plate 6, figs. 4–6
Distinguishing characters. Spherical to subspherical brown cysts with little to no polar compression. Central body thin walled, with verrucate ornamentation. Outer layer closely appressed to inner layer, supported by the verrucae and forming very slight ridges delineating the cingulum. Lines of verrucae may also distinguish the cingulum. A flagellar scar can be observed. Archeopyle theropylic, following cingulum, and operculum adnate ventrally. Based on Reid (1977).
Dimensions. Central body minimum diameter 35–44 µm, maximum diameter 37–51 µm (Reid, 1977).
Remarks. *Dubridinium ulsterum* differs from other species of *Dubridinium* in its irregular equatorial shape, size and strings of solid verrucate processes (Reid, 1977). The cysts withstand palynological treatment (Reid, 1977).
Biological affinity. Unknown.
Stratigraphic range. Modern sediments from the U.K. (Reid, 1977).

Genus *Gotoius* Abé, 1981
Comments. A motile-defined genus.

Cyst of *Gotoius abei* Matsuoka, 1988
Not illustrated here.
Distinguishing characters. Spherical to subspherical, dark brown cyst with a smooth wall. The archeopyle is large, theropylic and quadrate, delineated by two complete and two incomplete archeopyle sutures. Operculum is adnate and biplacoid; it is hinged at the plate boundaries between the 2a/2′–3′ and la/2′ plates and corresponds to the 2a and la plates. Based on Matsuoka (1988).
Dimensions. Cyst length 60 µm, width 52.5 µm (Matsuoka, 1988).
Remarks. It is not clear whether the cysts withstand palynological treatment.
Biological affinity. *Gotoius abei* according to Matsuoka (1988).
Stratigraphic range. Modern sediments from Yatsushiro Sea, Japan (Matsuoka, 1988).

Genus *Huia* Gu et al., 2016
Comments. A motile-defined genus.

Cyst of *Huia caspica* (Ostenfeld, 1902) Gu et al., 2016
Plate 6, figs. 7–9
Distinguishing characters. Spherical, brown, smooth-walled cysts. The archeopyle is theropylic, corresponding to the sutures between plates 2´, 1a, 3´ and 2´´, 3´, 4´´, 5´´. Based on Gu et al. (2016).
Dimensions. Cyst diameter 35.0–38.0 µm (Gu et al., 2016).
Remarks. It is unclear whether the cysts withstand palynological treatment.
Biological affinity. *Huia caspica* according to Gu et al. (2016).
Stratigraphic range. Modern sediments from the East China Sea (Gu et al., 2016).

Genus *Lebouraia* Abé, 1941 *ex* Sournia, 1986
Comments. A motile-defined genus.

Cyst of *Lebouraia pusilla* (Balech and Akselman, 1988) Dodge and Toriumi, 1993

Plate 6, figs. 10–12
Distinguishing characters. The cyst is spherical, pale brown and contains abundant granules. The archeopyle is theropylic and corresponds to the sutures of plate 1a. Based on Liu et al. (2015a).
Dimensions. Cyst body diameter 30.0–40.0 μm (Liu et al., 2015a).
Remarks. A similar cyst was described for the closely related species *Lebouraia minuta* Abé, 1941 by Sonneman and Hill (1997). The main difference between both thecate species lies in the fact that 1´ does not touch the anterior sulcal plate in *L. minuta*. Sonneman and Hill (1997) neither illustrate nor describe this feature, and therefore this cyst–theca relationship needs restudy. It is not clear whether the cysts withstand palynological treatment.
Biological affinity. *Lebouraia pusilla* based on Liu et al. (2015a).
Stratigraphic range. Modern sediments from the Yellow Sea and the South China Sea (Liu et al., 2015a).

Genus *Niea* Liu et al., 2015a
Comments. A motile-defined genus.

Cyst of *Niea acanthocysta* (Kawami et al., 2006) Liu et al., 2015a
Plate 7, figs. 1–3
Distinguishing characters. Cysts are spherical with a pale brown central body. The cyst surface is microgranular and bears fewer than 80 randomly distributed, slender, acuminate, solid and unpigmented processes with circular bases. The archeopyle is theropylic, formed by a zigzag split following the boundaries of 1a/2´´ (complete), 1a/3´´ (complete), 1a/4´´ (complete), 1a/5´´ (complete), 2´/2´´ (incomplete) and 3´/5´´ (incomplete). Based on Kawami et al. (2006), Mertens et al. (2015) and Liu et al. (2015a).
Dimensions. Central body diameter 30.0–53.0 μm, process length 1–8 μm (Kawami et al., 2006).
Remarks. The cysts withstand palynological treatment (Mertens et al., 2015). Mertens et al. (2015) remarked that this species resembles the cyst-defined species *Echinidinium transparatum* Zonneveld, 1997 ex Mertens et al., herein and *E. zonneveldiae* Head, 2003. However, *E. transparantum* is small and has long processes with rectangular bases and the archeopyle is a simple split. *E. zonneveldiae* has a theropylic archeopyle which forms a long straight split and has processes also with a rectangular base.
Biological affinity. *Niea acanthocysta* according to Kawami et al. (2006, as *Oblea acanthocysta*) and Liu et al. (2015a).
Stratigraphic range. Modern sediments from Omura Bay, Japan (Kawami et al., 2006) and the Yellow Sea, China (Liu et al., 2015a).

Cyst of *Niea chinensis* Liu et al., 2015a
Plate 7, figs. 4–6
Distinguishing characters. The cyst is spherical, brown in color and smooth-walled. The archeopyle is hexagonal and theropylic, corresponding to plate 1a. SEM shows that the cyst surface is finely ornamented. Based on Liu et al. (2015a).
Dimensions. Cyst diameter 25.0–50.0 μm (Liu et al., 2015a).
Remarks. It is not clear whether the cysts withstand palynological treatment.
Biological affinity. *Niea chinensis* according to Liu et al. (2015a).
Stratigraphic range. Modern sediments from the Yellow Sea, East China Sea and South China Sea (Liu et al., 2015a).

Cyst of *Niea torta* (Abé, 1941) Liu et al., 2015a
Plate 7, figs. 7–9
Distinguishing characters. The cyst is spherical, brown in color, with a finely and faintly ornamented surface. The archeopyle is theropylic, formed by a slit along the cingulum. Based on Liu et al. (2015a).
Dimensions. Cyst diameter 60.0–70.0 μm (Liu et al., 2015a).

Remarks. It is not clear whether the cysts withstand palynological treatment.
Biological affinity. *Niea torta* according to Liu et al. (2015a).
Stratigraphic range. Modern sediments from the Yellow Sea, China (Liu et al., 2015a).

Genus *Oblea* Balech, 1964 ex Loeblich Jr. and Loeblich III, 1966 emend. Liu et al., 2015
Comments. A motile-defined genus.

Cyst of *Oblea rotunda* (Lebour, 1922) Balech, 1964 ex Sournia, 1973
Plate 7, figs. 10–12
Distinguishing characters. Spherical, pale brown smooth-walled cysts. The archeopyle is theropylic, forming a split that extends about two thirds of the way around the cyst along the margin between the first intercalary (1a) plate and the second to fourth precingular plate, respectively. Living cysts contain pale droplets. Based on Lewis (1990).
Dimensions. Cyst diameter 22.0–31.0 μm (Lewis, 1990).
Remarks. It is not clear whether the cysts withstand palynological treatment.
Biological affinity. *Oblea rotunda* according to Lewis (1990) and Liu et al. (2015a).
Stratigraphic range. Modern sediments from the U.K. (Lewis, 1990) and the East China Sea and Yellow Sea, China (Liu et al., 2015a).

Genus *Qia* Liu et al., 2015a
Comments. A motile-defined genus.

Cyst of *Qia lebouriae* (Nie, 1943) Liu et al., 2015a
Plate 8, figs. 1–3
Distinguishing characters. Large brown cysts with spherical central body covered with numerous short hairs and/or solid spines that are curved distally. The archeopyle is theropylic and corresponds to plate 1a. Based on Liu et al. (2015a).
Dimensions. Cyst body diameter 45.0–60.0 μm, process length 3.1–10.0 μm (Liu et al., 2015a).
Remarks. The cysts withstand palynological treatment, as observed here.

Biological affinity. *Qia lebouriae* according to Liu et al. (2015a).
Stratigraphic range. Modern sediments from the Yellow Sea and South China Sea (Liu et al., 2015a) and from Omura Bay, Japan (this study).

Subfamily PROTOPERIDINIOIDEAE (Autonym)

Genus *Archaeperidinium* Jörgensen, 1912 emend. Yamaguchi et al., 2011
Comments. A motile-defined genus, that was reintroduced and emended by Yamaguchi et al. (2011).

Cyst of *Archaeperidinium bailongense* Liu et al., 2015b
Plate 8, figs. 4–6
Distinguishing characters. Cysts have a subspherical central body and are light brown in color when empty. Living cysts are darker brown and contain greenish granules. The central body wall is thin (>0.3 μm) with a granulate surface. Cysts are covered with slender, tapering, erect to recurved, apiculocavate processes with a narrow circular base, 1.0–2.4 μm in diameter, and capitate distal ends. Minute granules are present on the processes. The processes are mostly equal in length, with some smaller processes occasionally present. The density of process distribution is moderate, with four to seven processes per 10 × 10 μm. The processes are never fused or branched distally. The archeopyle is intercalary and theropylic and corresponds to the large 2a plate, the operculum remaining adnate along the boundary between 2a and precingular plates (Fig. 10). In palynologically treated samples, the operculum was sometimes observed detached. No flagellar scars. Based on Liu et al. (2015b).

Dimensions. Central body diameter 38.3–50.3 µm, process length 6.4–10.3 µm (Liu et al., 2015b).
Remarks. The cysts withstand palynological treatment, as observed here.
Biological affinity. *Archaeperidinium bailongense* according to Liu et al. (2015b).
Stratigraphic range. Modern sediments from the South China Sea (Liu et al., 2015b).

Cyst of *Archaeperidinium constrictum* (Abé, 1936) Liu et al., 2015b
Plate 8, figs. 7–9
Distinguishing characters. Cysts have a subspherical central body and are light brown in color when empty. Live cysts are darker brown and contain greenish granules. The central body wall is thin (>0.3 µm) with a smooth surface. Cysts are covered with slender, tapering, erect, apiculocavate processes with wide circular bases, 1.4–2.4 µm in diameter, and capitate distal ends. The processes are smooth and mostly equal in length, with some shorter processes being occasionally present. The density of the processes varies between moderate and high, with 19–37 processes per 10 × 10 µm. When the density is very high, adjacent process bases contact one another. The processes are never fused or branched distally. The archeopyle is theropylic, corresponding to the large 2a plate. Based on Liu et al. (2015b).
Dimensions. Central body diameter 28.1–47.6 µm, process length 3.8–6.4 µm (Liu et al., 2015b).
Remarks. The cysts withstand palynological treatment, as observed here.
Biological affinity. *Archaeperidinium constrictum* according to Liu et al. (2015b).
Stratigraphic range. Modern sediments from the Yellow Sea, China (Liu et al., 2015b) and Omura Bay, Japan (this study), as well as sediment trap samples from the Cariaco Basin (Bringué et al., 2019).

Cyst of *Archaeperidinium minutum* (Kofoid, 1907) Jörgensen, 1912 sensu stricto
Plate 8, figs. 10–12
Distinguishing characters. Cysts have a spherical to subspherical central body and are dark brown when cell contents are present and light brown when empty. Empty cysts also appear darker when covered in mucus. The living cysts have abundant reddish granules. The wall is thin. The central body surface is smooth and densely packed with numerous equidistant, non-tabular, processes (20–30 processes per 10 × 10 µm). Under light microscopy, the processes appear distally solid with pericoels extending a variable distance along process shaft. Small bumps are sometimes observed between processes, and may be arranged in a polygonal pattern around the process bases similar to the polygonal patterns observed on the theca of *Protoperidinium minutum* (Dodge, 1983, his fig. 8). Processes are erect and taper to acuminate or minutely expanded tips. The SEM illustration on Plate 8, fig. 12 shows minutely bifurcate tips with recurved branches. The processes are never fused. The process bases are circular in cross-section. The archeopyle, which is the only expression of tabulation on the cyst, is intercalary and theropylic and corresponds to the 2a plate. Based on Mertens et al. (2012b).
Dimensions. Central body diameter 24.0–33.1 µm, process length 3.4–7.2 µm (Mertens et al., 2012b).
Remarks. The cysts withstand palynological treatment (Mertens et al., 2012b). Very similar cysts that have been related to the same motile stage have been described by Fukuyo et al. (1977) and Ribeiro et al. (2010); it is unclear whether these constitute separate species or not (see Mertens et al., 2012b, p. 59).
Biological affinity. *Archaeperidinium minutum* according to Mertens et al. (2012b).
Stratigraphic range. Modern sediments off Portugal (Ribeiro et al., 2010), Yellow Sea of China (Liu et al., 2015b) and Vancouver Island (Mertens et al., 2012b).

Cyst of *Archaeperidinium minutum* (Kofoid, 1907) Jörgensen, 1912 sensu Wall and Dale, 1968
Plate 9, figs. 1–3
Distinguishing characters. Cysts have a spherical central body, are brown in color, and the minutely undulating central body wall bears approximately forty short hollow processes with circular bases and more or less flat-topped distal extremities. The outer rims of the extremities of these processes bear tapering spinules that may be minutely expanded distally (Plate 9, fig. 3). The intercalary archeopyle (?1a or 2a), rarely clearly discernible, is subtrapezoidal to subrectangular in shape with a length to breadth

ratio of around 0.6. The cell contents are often dense and include numerous plastids. Based on Wall and Dale (1968).
Dimensions. Central body diameter 41–43 µm, process length 7–9 µm, archeopyle about 17 × 28 µm (Wall and Dale, 1968).
Remarks. The cysts withstand palynological treatment (e.g., Pospelova et al., 2005).
Biological affinity. *Archaeperidinium minutum* according to Wall and Dale (1968) but is probably a closely related species given that a markedly different cyst type has been related to the same species (see above).
Stratigraphic range. Modern sediments from Woods Hole waters (Wall and Dale, 1968), Buzzards Bay (Massachusetts, USA) (Pospelova et al., 2005) and Baie de Vilaine, France (this study).

Cyst of *Archaeperidinium monospinum* (Paulsen, 1907) Jorgensen, 1912
Plate 9, figs. 4–6
Distinguishing characters. Cysts have a subspherical central body, and are pale brown in color with grey-brown cell content. The central body bears numerous randomly distributed processes of two types. One type is longer, hollow and minutely expanded or bifurcated at the distal end. The other type is solid, acuminate and scattered randomly between the longer processes. The archeopyle is theropylic and corresponds to the large 2a plate, the operculum remaining adnate. Based on Zonneveld and Dale (1994) and observations made here.
Dimensions. Central body diameter 28–40 µm, hollow processes 3–7 µm long, solid spines about 3 µm long (Zonneveld and Dale, 1994).
Remarks. The cysts withstand palynological treatment, as observed here.
Biological affinity. *Archaeperidinium monospinum* according to Zonneveld and Dale (1994).
Stratigraphic range. Modern sediments from Oslo fjord (Zonneveld and Dale, 1994) and French estuaries (this study).

Cyst of *Archaeperidinium saanichi* Mertens et al., 2012b
Plate 9, figs. 7–9
Distinguishing characters. Cysts have a spherical to subspherical central body, and are dark brown when cell content is present and hazel brown when empty. The living cysts have abundant orange granules. The central body wall is thin with a smooth surface densely packed with numerous equidistant, non-tabular processes (15–22 processes per 10×10 µm). Bumps or reduced processes may be observed between processes. Processes are tapering, hollow and generally erect but can be slightly inflected, and always end in minute distal expansions. The processes are never fused or branched at their ends. The process bases are circular in cross-section. The archeopyle is intercalary and theropylic and corresponds to the large 2a plate. Based on Mertens et al. (2012b).
Dimensions. Central body diameter 36.0–52.0 µm, process length 2.8–7.8 µm (Mertens et al., 2012b).
Remarks. The cysts withstand palynological treatment (Mertens et al., 2012b).
Biological affinity. *Archaeperidinium saanichi* according to Mertens et al. (2012b).
Stratigraphic range. Upper Quaternary to modern sediments from the Santa Barbara Basin and California margin (Bringué et al., 2014; Pospelova et al., 2015) and modern sediments from Vancouver Island (Mertens et al., 2012b).

Genus *Brigantedinium* Reid, 1977 ex Lentin and Williams, 1993
Comments. A cyst-defined genus.

Brigantedinium asymmetricum Matsuoka, 1987 ex Head, 1996
Plate 9, figs. 10–12
Distinguishing characters. Small spherical brown cyst, surface microgranular (not smooth as described by Matsuoka, 1987). Archeopyle intercalary, saphopylic, relatively large, and comprising one long, two intermediate, two short and one convex side. Based on Matsuoka (1987).

Dimensions. Cyst diameter 30.0–32.8 µm (Matsuoka, 1987).
Remarks. The cysts withstand palynological treatment (Matsuoka, 1987). Matsuoka (1987) remarked that this spherical cyst resembles *Brigantedinium cariacoense* in bearing a curved margin along the principal archeopyle suture, but differs in that its archeopyle is irregularly hexagonal in shape. Specimens of *Protoperidinium* sp. cf. *conicoides* are similar to the present species and were recorded from modern California Current surface sediments by Wall (1986).
Biological affinity. Unknown.
Stratigraphic range. Modern sediments from Akkeshi Bay, Hokkaido, Japan (Matsuoka, 1987) and Lake Saroma, Japan (this study).

Brigantedinium auranteum Reid, 1977 ex Lentin and Williams, 1993
Plate 10, figs. 1–3
Distinguishing characters. Spherical, pale brown, smooth and thick-walled cysts. Archeopyle large, saphopylic, subhexagonal, its longest axis up to three fifths of the cyst diameter with a length/breadth ratio of 1:1. Based on Reid (1977).
Dimensions. Cyst length 42–58 µm, width 40–63 µm, archeopyle length 26–30 µm, width 26–30 µm, wall thickness 1–2.5 µm (Reid, 1977).
Remarks. The cysts withstand palynological treatment (Reid, 1977).
Biological affinity. Unknown.
Stratigraphic range. Modern sediments from the U.K. (Reid, 1977) and Saanich Inlet, B.C., Canada (this study).

Brigantedinium majusculum Reid, 1977 ex Lentin and Williams, 1993
Plate 10, figs. 4–6
Distinguishing characters. Large, spherical, dark brown, smooth and thick-walled cysts. Archeopyle intercalary, saphopylic, hexagonal, its anterior suture (with the apical plate series) sub-parallel to its posterior suture which is the longest. Two long lateral sutures diverge antapically from the apical suture by short converging sutures. Based on Reid (1977).
Dimensions. Cyst diameter 73–92 µm, archeopyle length 39–39, width 32–23 µm (Reid, 1977).
Remarks. The cysts withstand palynological treatment (Reid, 1977).
Biological affinity. *Protoperidinium sinuosum* according to Li et al. (2015b).
Stratigraphic range. Upper Pleistocene of the Northern and Western Pacific (Bujak and Matsuoka, 1986), Holocene sediments off Korea (Shin et al., 2010b) and off West Greenland (Ribeiro et al., 2012b), and modern sediments from the U.K. (Reid, 1977), from Tongyeong coastal area, Korea (this study) and Izmir Bay, Turkey (this study).

Genus *Cristadinium* Head et al., 1989
Comments. A cyst-defined genus.

Cristadinium striatiserratum Uddandam et al., 2018
Plate 10, figs. 7–9
Distinguishing characters. Peridinioid cyst, light brown in color and pentagonal in outline. Conical epicyst with thickened apical structure. The hypocyst bears two symmetrical antapical horns with distal acuminate spines or rounded horns. Cingulum pronounced. Sulcus widens towards the antapex. Archeopyle formed by loss of the second intercalary plate. Based on Harland (1977) and Uddandam et al. (2018).
Dimensions. Cyst length 55.0–62.5 µm, width, 57.5–68.7 µm (Harland, 1977).
Remarks. Specimens illustrated by Harland (1977, as *Lejeunecysta paratenella*) are assigned to *Cristadinium striatiserratum*, differing from *Lejeunecysta paratenella* described by Benedek (1972) which has denticulate margins. The cysts withstand palynological treatment (Harland, 1977).
Biological affinity. *Protoperidinium* sp. according to Harland (1977).

Stratigraphic range. Upper Quaternary of the U.K. (Harland, 1977) and Cariaco Basin (Mertens et al., 2009) and modern sediments from Japan (Kojima, 1989), the Arabian Sea (D'Silva et al., 2011; Uddandam et al., 2018) and Myanmar (Su-Myat, 2012).

Genus *Islandinium* Head et al., 2001
Comments. A cyst-defined genus.

Islandinium pacificum Gurdebeke et al., 2019
Plate 10, figs. 10–12
Distinguishing characters. Light brown cyst with a spherical central body, its smooth wall bearing numerous randomly distributed processes. Processes are apiculocavate, erect or recurved, slender, acuminate, and harpoon-like, bearing fine barbs. Archeopyle saphopylic A3, with no other reflections of tabulation on the cyst. Based on Gurdebeke et al. (2019).
Dimensions. Central body diameter 28.9 (35.7) 42.2 µm, process length 7.4 (10.4) 12.7 µm (Gurdebeke et al., 2018).
Remarks. The cysts withstand palynological treatment (Gurdebeke et al., 2019). *Islandinium pacificum* resembles *Islandinium minutum* subsp. *barbatum* Potvin et al. (2018) both in size range and nature of the processes, but is distinguished by the surface texture of the central body wall (smooth vs. faintly to prominently granulate).
Biological affinity. *Protoperidinium mutsuense* according to Gurdebeke et al. (2019).
Stratigraphic range. Last Interglacial of the North Atlantic, and Upper Pleistocene and Holocene including modern sediments from the northeastern Pacific (Gurdebeke et al., 2019).

Genus *Leipokatium* Bradford, 1975
Comments. A cyst-defined genus.

Leipokatium invisitatum Bradford, 1975
Plate 11, figs. 1–2
Distinguishing characters. Peridinioid cyst with large epicyst and small hypocyst. Epicyst domed or conical with or without an apical horn or apical wall thickening. Cingulum broad equatorially: hypocyst very small, usually dorsoventrally compressed, with or without antapical horns. Polar view circular to reniform with small sulcal depression. Wall thin, usually smooth or lightly ornamented. Anterior intercalary archeopyle. Based on Bradford (1975).
Dimensions. Cyst length 31–56 µm, lateral width 37–80 µm, dorsoventral width 45 µm, archeopyle height 9–15 µm, archeopyle width 14–27 µm, length of antapical horns 10–21 µm, distance between antapical horns (distally) 10–30 µm (Bradford, 1975).
Remarks. The cysts withstand palynological treatment (Bradford, 1975).
Biological affinity. Unknown.
Stratigraphic range. Middle Miocene off New Jersey (de Verteuil, 1996), and modern sediments from the Persian Gulf (Bradford, 1975) and the South China Sea (this study).

Genus *Lejeunecysta* Artzner and Dörhöfer, 1978 emend. Lentin and Williams, 1976
Comments. A cyst-defined genus.

Lejeunecysta? *epidoma* Matsuoka, 1987
Plate 11, figs. 3–6
Distinguishing characters. Large, light orange brown cysts, with a smooth to finely granular surface. Epicyst broad, dome-shaped without apical boss. Hypocyst large, trapezoidal outline in dorsoventral view, possessing two very small antapical horns with thickened distal tips. Cingulum indicated by indentation of autophragm with some longitudinal striations. Shallow sulcus which sometimes shows

flagellar scars. Archeopyle hexagonal intercalary, with four long and two short principal archeopyle sutures (steno-delta form). Based on Matsuoka (1987).
Dimensions. Cyst length 74.6–84.0 µm, width 74.6–80.0 µm, width of the cingulum ca. 8 µm (Matsuoka, 1987).
Remarks. The cysts withstand palynological treatment (Matsuoka, 1987).
Biological affinity. Unknown, but probably *Protoperidinium* sp. (Conica group) according to Matsuoka (1987).
Stratigraphic range. Modern sediments from Akkeshi Bay, Japan (Matsuoka, 1987).

Lejeunecysta marieae (Harland in Harland et al., 1991) Lentin and Williams, 1993
Plate 11, figs. 7–9
Distinguishing characters. Peridinioid cysts that are light brown in color. Wall surface is moderately to faintly granulate under LM, under SEM the surface bears granules/gemmae (0.5 um or less in diameter) which are themselves covered in minute (<0.1 µm) granules that densely cover entire surface. Blunt spines less than 1.0 µm high occur along cingular margins and may also be present elsewhere. Epicyst longer than hypocyst, conical and with convex sides. Apical horn weakly developed and indicated by a slightly thickened (<1.5µm) apical boss. Hypocyst outline rounded trapezoidal in dorsoventral view, with two equally developed antapical horns that are moderately to strongly divergent and bear solid, acuminate tips. Cingulum fairly pronounced and indicated by transverse folding. Sulcus is shallow. Archeopyle intercalary hexa 2a isodeltaform with short H3 and H5 sides; operculum free, sometimes adherent on adcingular margin. There are no other indications of tabulation. Based on Head (1993).
Dimensions. Cyst length 34–50 µm (Harland et al., 1991) and 27–47 µm (Head, 1993); width 27–38 µm, antapical horn tip length (from base of solid thickening) 1.7–5.7 µm (Head, 1993).
Remarks. The cysts withstand palynological treatment (Harland et al., 1991).
Biological affinity. Unknown.
Stratigraphic range. Langhian (Middle Miocene) of Austria and Hungary (Jiménez-Moreno et al., 2016), Middle to Upper Miocene off New Jersey (de Verteuil, 1996), Lower Pleistocene of the U.K. (Head, 1993), upper Quaternary of the Cariaco Basin (Mertens et al., 2009), and modern sediments from northeastern USA (Pospelova et al., 2004, 2005; Price et al., 2016, as *Lejeunecysta oliva*) and Nova Scotia (this study). Questionably recorded from the Burdigalian (Lower Miocene) of Austria (Jiménez-Moreno et al., 2016).

Genus *Protoperidinium* Bergh, 1881b
Comments. A motile-defined genus.

Cyst of *Protoperidinium abei* (Paulsen, 1931) Balech var. *rotundata* (Abé, 1936) Taylor, 1976
Plate 11, figs. 10–12
Distinguishing characters. Cysts are spherical, dark brown, with a granulate surface. No flagellar scars were observed. The archeopyle is hexagonal, asymmetrical and saphopylic, reflecting the shape of 1a; the suture between 1a and 2´ is more nearly parallel to the suture between 1a and 3´´ than the suture between 1a and 2a. Based on Liu et al. (2015b).
Dimensions. Cyst diameter 50.0–55.0 µm (Liu et al., 2015b).
Remarks. It is not clear whether the cysts withstand palynological treatment. Liu et al. (2015b) remarked that the cyst of *Protoperidinium abei* var. *rotundata* is very similar to *Brigantedinium cariacoense*, the only difference being its significantly larger diameter (50–55 µm compared to 30–35 µm). *Brigantedinium irregulare* Matsuoka, 1987 ex Head, 1996 is presumably the same species; incubation experiments from the type locality would be needed to confim this relationship.
Biological affinity. *Protoperidinium abei* var. *rotundata* according to Liu et al. (2015b).
Stratigraphic range. Modern sediments from the Yellow Sea and the East China Sea (Liu et al., 2015b).

Cyst of *Protoperidinium biconicum* (Dangeard, 1927) Balech, 1974

Plate 12, figs. 1–3
Distinguishing characters. Biconical cysts, circular in apical view and dark brown in color when empty. The epicyst and hypocyst are equal in length. The cyst wall is smooth, lacking striations. The blunt apical horn is less wide than the blunt antapical horn. The sides of epi- and hypocyst are concave. There is a strongly developed, wide (8.8–13.1 μm) cingulum formed by two parallel ridges. The archeopyle has rounded margins, is iso-deltaform-linteloid (hexa), located in the epicyst and offset to the left of the dorsal midline, probably corresponding to plate 2a. The operculum is free. A flagellar scar is clearly visible in the sulcus. Based on Gu et al. (2015b).
Dimensions. Cyst length 60.6–75.0 μm, width 75.0–90.0 μm, depth 75.0–87.0 μm, archeopyle length 29.5–37.0 μm, width 25.0–29.0 μm (Gu et al., 2015b).
Remarks. The cysts withstand palynological treatment, as observed here. Gu et al. (2015a) remarked that the cyst of *Protoperidinium biconicum* had previously been reported as *Peridinium* sp. 2 (Wall and Dale, 1968, plate 4, figure 10) and is morphologically similar to *Selenopemphix nephroides* but the hypocyst narrows more conspicuously towards the antapex. *Selenopemphix alticinctum* is considerably smaller (holotype width 39 μm; Bradford, 1975) and like *S. nephroides* has a broader antapex.
Biological affinity. *Protoperidinium biconicum* according to Gu et al. (2015b).
Stratigraphic range. Modern sediments of the South China Sea (Gu et al., 2015b).

Cyst of *Protoperidinium denticulatum* (Gran and Braarud, 1935) Balech, 1974
Plate 12, figs. 4–6
Distinguishing characters. Spherical, darker brown, smooth-walled cysts with a saphopylic, equatorially elongate, hexagonal, intercalary archeopyle. Based on Wall and Dale (1968).
Dimensions. Cyst diameter 56 μm, archeopyle 21 × 36 μm (Wall and Dale, 1968).
Remarks. The cysts withstand palynological treatment using warm HF (Konieczny, 1983). *Brigantedinium grande* Matsuoka, 1987 ex Head, 1996 is potentially the cyst stage of this species, which has a similar size; the type locality of the cyst stage should be restudied to confirm the cyst–theca relationship.
Biological affinity. *Protoperidinium denticulatum* according to Wall and Dale (1968).
Stratigraphic range. Modern sediments from Woods Hole, U.S.A. (Wall and Dale, 1968), Akkeshi Bay, Japan (Matsuoka, 1987), Bohai Sea (Liu et al., 2015b) and Norway (this study).

Cyst of *Protoperidinium excentricum* (Paulsen, 1907) Balech, 1974
Plate 12, figs. 7–9
Distinguishing characters. Cysts pale brown, smooth-walled, and apical–antapically compressed. They have an indented sulcus and are often enclosed by an outer layer reflecting thecal features. The archeopyle is theropylic and follows the sutures between 2′, 3′ and 2a, and 2″, 1a, 4″, 5″, and 6″, respectively. Based on Lewis et al. (1984) and Liu et al. (2015b).
Dimensions. Central body length 30.0–52.9 μm, width 50.0–70.0 μm, depth 38.5–47.0 μm (Liu et al., 2015b).
Remarks. It is not clear whether the cysts withstand palynological treatment.
Biological affinity. *Protoperidinium excentricum* according to Wall and Dale (1968) and Lewis et al. (1984).
Stratigraphic range. Modern sediments from Woods Hole (Wall and Dale, 1968) the U.K. (Lewis et al., 1984), off Argentina (Akselman, 1987), and Denmark (Ellegaard et al., 1994).

Cyst of *Protoperidinium fukuyoi* Mertens et al., 2013
Plate 12, figs. 10–12
Distinguishing characters. Cysts have a spherical to subspherical central body and light brown to golden brown color. Cell contents are typically colorless. The central body surface is smooth to finely and faintly granulate, bearing numerous erect, flattened, straight to curved processes that taper to acuminate or blunt tips. Processes are typically clustered in straight or arcuate linear complexes, but some are distributed

irregularly over the entire cyst. The archeopyle is angular, apical, and saphopylic, comprising release of plates Po, X, 2′, 3′ and 4′. Based on Mertens et al. (2013).
Dimensions. Central body maximum diameter, 23.0–34.6 μm, process length, 1.9–7.4 μm (Mertens et al., 2013).
Remarks. The cysts withstand palynological treatment (Mertens et al., 2013).
Biological affinity. *Protoperidinium fukuyoi* according to Mertens et al. (2013).
Stratigraphic range. Upper Quaternary of the Santa Barbara Basin (Pospelova et al., 2006, as cyst type A) and California margin (Pospelova et al., 2015), and modern sediments over a long stretch of the northeastern Pacific shelf (Mertens et al., 2013).

Cyst of *Protoperidinium fuzhouense* Liu et al., 2015b
Plate 13, figs. 1–3
Distinguishing characters. Cysts are spherical and dark brown. Living cysts contain greenish granules. At the antapex, a septum demarcates one pentagonal antapical plate (reflecting 1′′′′) surrounded by five incomplete plates. The cyst surface is coarse and covered with granules, with a theropylic archeopyle along the sutures between 1a and 2′′, 2′, 3′, and 2a. Only one cyst was isolated and yielded motile cells upon germination. Based on Liu et al. (2015b).
Dimensions. Cyst diameter 44 μm (Liu et al., 2015b).
Remarks. It is not clear whether the cysts withstand palynological treatment.
Biological affinity. *Protoperidinium fuzhouense* according to Liu et al. (2015b).
Stratigraphic range. Modern sediments of the East China Sea (Liu et al., 2015b).

Cyst of *Protoperidinium humile* (Schiller, 1935) Balech, 1974
Plate 13, figs. 4–5
Distinguishing characters. Cysts are light brown when empty, are reniform in polar view due to an invagination of the sulcus, and rounded in ventral view. The epicyst is much wider than the hypocyst and extends to the dorsal surface. Living cysts are dark brown and contain many transparent granules. The wall bears striations. The archeopyle is hexagonal, saphopylic, offset to the left of the dorsal midline, has sharp angles, and corresponds to the 3a plate. Based on Gu et al. (2015b).
Dimensions. Cyst length 55.0–65.0 μm, width 60.0–70.0 μm, depth 30.0–43.0 μm, archeopyle length 20.6–29.6 μm, width 13.1–19.8 μm (Gu et al., 2015b).
Remarks. It is not clear whether the cysts withstand palynological treatment.
Biological affinity. *Protoperidinium humile* according to Gu et al. (2015b).
Stratigraphic range. Modern sediments from Yellow Sea and South China Sea (Gu et al., 2015b).

Cyst of *Protoperidinium latissimum* (Kofoid, 1907) Balech, 1974
Plate 13, figs. 6–9
Distinguishing characters. Orange brown cysts that are large, peridinioid, smooth-walled, and dorsoventrally compressed, and concavoconvex to hemispherical in polar view, and elliptical in lateral view. The dorsal surface is strongly convex and the ventral surface is concave or almost straight at the equator, where the cingulum is reflected only by two broad lateral lobes that are weakly excavated and support two small apophyses each. The epicyst and hypocyst are similar in size. The epicyst tapers strongly to a blunt apical horn and has concave sides. The intercalary archeopyle (2a) is subtriangular with briefly truncated angles. The hypocyst tapers rapidly away from the cingulum towards the antapex, which either is straight-based or indented to form two small pointed horns. Based on Wall and Dale (1968).
Dimensions. Cyst length 65–100 μm, width 56–85 μm, depth 32–43 μm, archeopyle length 19–24 μm, width 28–44 μm (Wall and Dale, 1968).
Remarks. The cysts withstand palynological treatment (Matsuoka, 1985). The cyst-defined species *Quinquecuspis chinensis* He Chengquan and Sun Xuekun, 1991 ex He Chengquan et al., 2009 is a very similar cyst, although larger (length 118.2–124.9 μm, width 93.6–94.0 μm).

Biological affinity. *Protoperidinium latissimum* (Kofoid, 1907) Balech, 1974, according to Wall and Dale (1968), Sonneman and Hill (1997), and Gu et al. (2015b).
Stratigraphic range. Holocene sediment from the South China Sea (Li et al., 2017) and modern sediments from Woods Hole, U.S.A. (Wall and Dale, 1968), Nagasaki Bay, Japan (Matsuoka, 1985), Australia (Sonneman and Hill, 1997), South Korea (this study) and the Yellow Sea, China (Gu et al., 2015b).

Cyst of *Protoperidinium lewisiae* Mertens et al., 2015
Plate 13, figs. 10–12
Distinguishing characters. Cysts brown in color with a spherical to subspherical central body. Living cysts have abundant greenish pigments and endospore. The wall is thin, and the surface microgranular, covered with more-or-less equidistant, short to long, slender, erect (more often curved when long), apiculocavate processes that are never fused and terminate in acuminate tips. These processes have circular to ovoidal proximal bases, and carry many minute spinules, which are difficult to observe under LM but are clearly seen under SEM. There are 8–20 processes per 10 × 10 μm. Generally, more processes occur on specimens with shorter processes. The archeopyle is theropylic, following the cingulum. Based on Mertens et al. (2015).
Dimensions. Central body diameter 25.7–33.6 μm, process length 3.6–7.2 μm.
Remarks. The cysts withstand palynological treatment (Mertens et al., 2015). Cysts of *Protoperidinium lewisiae* were described as Dinoflagellate cyst type B in Matsuoka (1987, his pl. 18, figs. 5–8). Cysts of *Protoperidinium lewisiae* would fit into the cyst-defined genus *Echinidinium* because of their theropylic archeopyle.
Biological affinity. *Protoperidinium lewisiae* according to Mertens et al. (2015).
Stratigraphic range. Modern sediments from Lake Saroma, Japan, Changle Harbor, East China Sea, China and Jinzhou Harbor, Bohai Sea, China, and San Pedro Harbor, California, U.S.A. (Mertens et al., 2015).

Cyst of *Protoperidinium parthenopes* Zingone and Montresor, 1988
Plate 14, figs. 1–3
Distinguishing characters. Cyst spherical, capsulate, and pale brown in color; wall bilayered, pericoel entirely surrounds central body with average height of 5.4 μm. Outer layer thin, smooth, pale brownish-orange in color; continuous over central body. Some parts of outer layer fold sharply, appearing as meandering lines over surface of central body. Lines do not correspond to tabulation. Inner layer thicker (ca. 0.4 μm), granulate outer surface, pale brown in color. Three polygonal plates observed on endocyst surface; archeopyle essentially saphopylic, formed along periphery of these three plates. Some plates may remain on cyst apparently due to conditions immediately following excystment. Based on Kawami and Matsuoka (2009).
Dimensions. Central body diameter 24–34 μm (Kawami and Matsuoka, 2009).
Remarks. This cyst type was considered not to survive palynological preparation; but specimens have been observed to withstand this treatment.
Biological affinity. *Protoperidinium parthenopes* according to Kawami and Matsuoka (2009).
Stratigraphic range. Modern sediments from Omura Bay, Japan (Kawami and Matsuoka, 2009).

Cyst of *Protoperidinium punctulatum* (Paulsen, 1907) Balech, 1974
Plate 14, figs. 4–6
Distinguishing characters. Large dark brown spherical cysts with a relatively large, saphopylic 2a intercalary archeopyle. The archeopyle is hexagonal, elongate equatorially with a length:breadth ratio around 0.6, and asymmetrical. Based on Wall and Dale (1968).
Dimensions. Cyst diameter 52–65 μm, archeopyle 20–30 μm (Wall and Dale, 1968).
Remarks. None.

Biological affinity. *Protoperidinium punctulatum* according to Wall and Dale (1968), Dobell (1978), Ellegaard et al. (1994) and Sonneman and Hill (1997). The cysts withstand palynological treatment using warm HF (Konieczny, 1983).
Stratigraphic range. Modern sediments from Woods Hole (Wall and Dale, 1968), British Columbia, Canada (Dobell, 1978), Denmark (Ellegaard et al., 1994) and Australia (Sonneman and Hill, 1997).

Cyst of *Protoperidinium thorianum* (Paulsen, 1905) Balech, 1973
Plate 14, figs. 7–9
Distinguishing characters. Cysts spherical, smooth-walled, and dark brown. The archeopyle is saphopylic and corresponds to the first or second intercalary plate. The operculum, although broadly resembling that of *Brigantedinium cariacoense*, does not have a pronounced curved margin. Based on Lewis et al. (1984) and Sonneman and Hill (1997).
Dimensions. Cyst diameter 50–55 µm (Lewis et al., 1984).
Remarks. It is not clear whether the cysts withstand palynological treatment. It is most similar to the cysts of *Protoperidinium denticulatum* but differs in the shape of the archeopyle.
Biological affinity. *Protoperidinium thorianum* according to Dobell (1978), Lewis et al. (1984) and Sonneman and Hill (1997).
Stratigraphic range. Modern sediments from British Columbia, Canada (Dobell, 1978), the U.K. (Lewis et al., 1984), Australia (Sonneman and Hill, 1997), and Bantry, Ireland (this study).

Cyst of *Protoperidinium thulesense* (Balech, 1958) Balech, 1973
Plate 14, figs. 10–12
Distinguishing characters. Cysts brown, spherical and smooth walled. The theropylic archeopyle is a large slit with a smooth or slightly zigzag suture. It is located equatorially, and encircles approximately two-thirds to three-quarters of the circumference of the cell. Sometimes one or two flagellar scars are observed on the side opposite the archeopyle. Based on Matsuoka et al. (2006).
Dimensions. Cyst diameter 33–50 µm (Matsuoka et al., 2006).
Remarks. It is not clear whether the cysts withstand palynological treatment.
Biological affinity. *Protoperidinium thulesense* according to Matsuoka et al. (2006).
Stratigraphic range. Modern sediments from Omura Bay, Japan (Matsuoka et al., 2006).

Cyst of *Protoperidinium tricingulatum* Kawami et al., 2009
Plate 15, figs. 1–3
Distinguishing characters. Cysts with spherical central body bearing numerous slender processes randomly distributed over the surface. The central body wall is light brown in color and its surface is smooth to slightly granular. The processes are apiculocavate and capitate or cauliforate. Process bases are circular in cross section. There are approximately 15 processes per 10 × 10 µm. The archeopyle is theropylic, with sutures probably corresponding to thecal plate boundaries of 2′/1a (complete), 2′/2a (complete), 3′/2a (complete), 4′/2a (complete), 4′/6″ (incomplete) and 4′/7″ (incomplete?), because the sutures that make the characteristic quadrant on the surface of some specimens give the same shape as the third apical plate. Based on Kawami et al. (2009).
Dimensions. Central body diameter 27–34 µm, process length 5–7 µm, wall thickness 0.8 µm (Kawami et al., 2009).
Remarks. The cysts withstand palynological treatment, as observed here.
Biological affinity. *Protoperidinium tricingulatum* according to Kawami et al. (2009).
Stratigraphic range. Modern sediments Huibertsplaat in the Wadden Sea off the coast of the Netherlands (Kawami et al., 2009) and from Saroma Lake, Japan (this study).

Genus *Selenopemphix* Benedek, 1972 emend. Head, 1993 nom. cons.
Comments. A cyst-defined genus. *Selenopemphix* Benedek, 1972 is conserved against the genus *Margosphaera* Nagy, 1965 (Fensome et al., 2016).

Selenopemphix tholus (Bradford, 1975) Head, 1996
Plate 15, figs. 4–6
Distinguishing characters. Cysts pentagonal in ambitus, circular, ovoidal, or reniform in polar view. Epicyst and hypocyst of similar size. Epicyst with or without apical horns or wall thickening; flanks of epicyst concave, apex domed or conical. Hypocyst with or without two antapical horns or antapical wall thickenings; phragma concave. Cysts broaden significantly in equatorial zone; cingulum extremely narrow. Sulcus distinct. Large, hoof-shaped intercalary archeopyle. Surface usually smooth and wall thin. Based on Bradford (1975).
Dimensions. Cyst length 46–50 µm, width 56–68 µm, archeopyle height 21–29 µm, archeopyle width 23–24 µm, width of antapical flange 16–19 µm (Bradford, 1975).
Remarks. The cysts withstand palynological treatment (Bradford, 1975).
Biological affinity. *Protoperidinium* sp. according to Wall and Dale (1968, as *Peridinium* sp.).
Stratigraphic range. Upper Oligocene of Argentina (Palamarczuk et al., 2000) to modern sediments from the Persian Gulf (Bradford, 1975), Kingston Harbour, Jamaica (Wall and Dale, 1968) and Sasebo Bay, Japan (this study).

Selenopemphix undulata Verleye et al., 2011
Plate 15, figs. 7–9
Distinguishing characters. A large cyst with a pale to medium brown color and a reniform, subcircular to circular ambitus in polar view. The epicyst is conical and the hypocyst carries distally two weakly developed rounded horns. Strongly developed and wide cingulum formed by two parallel ridges, with slightly thickened and undulating margins. The large rounded archeopyle is formed by loss of the 2a plate and offset to the left of the dorsal midline. The operculum is free. Based on Verleye et al. (2011).
Dimensions. Cyst width 49.5–89.4 µm, depth 37.9–82.3 µm; archeopyle width 16.9–38.4 µm; archeopyle height 12.0–24.3 µm (Verleye et al., 2011).
Remarks. The cysts withstand palynological treatment (Verleye et al., 2011). *Selenopemphix nephroides* is distinguished from *Selenopemphix undulata* by the smooth cyst wall and the absence of undulated cingular margins. Mertens et al. (2017) genetically sequenced the cyst and showed that it is closely allied with *Protoperidinium biconicum*.
Biological affinity. Unknown.
Stratigraphic range. Upper Quaternary of Santa Barbara Basin and offshore Chile, including modern sediments from the northeastern Pacific, southeastern Pacific and northwestern Pacific (Verleye et al., 2011).

Genus *Stelladinium* Bradford, 1975
Comments. A cyst-defined genus. See Head et al., this issue.

Stelladinium abei Matsuoka, 1985 subsp. *abei* (autonym)
Plate 15, figs. 10–12
Distinguishing characters. Orange brown, peridinioid cyst bearing one conspicuous apical and two symmetrical and conical antapical horns. Cyst body is compressed dorsoventrally except for the cingular regions. Cingulum lacks horn-like projections and is represented by projected shelf of the autophragm, transversely surrounding the cyst body. Sulcal area is suggested by moderate indentation. Archeopyle is apparently trapezoidal with four long and two short margins, and formed by loss of the 2a plate. Operculum is probably free. Based on Matsuoka (1985).
Dimensions. Cyst length 40 µm, width 44 µm (Matsuoka, 1985).
Remarks. The cysts withstand palynological treatment (Matsuoka, 1985).
Biological affinity. *Protoperidinium* sp. according to Matsuoka (1985).
Stratigraphic range. Upper Pleistocene of Japan (Bujak and Matsuoka, 1986) to modern sediments from Senzaki Bay, Japan (Matsuoka, 1985).

Stelladinium bifidum Head et al., this issue
Plate 16, figs. 1–3
Distinguishing characters. Cysts brown in color, peridinoid in outline, with long apical and antapical horns of approximately equal length, tapering from relatively narrow bases. Wall appears finely and faintly granulate owing to relief on the inside of the wall. Cingulum represented by a broad fold bearing numerous processes both on the dorsal and ventral surfaces and on lateral margins. Processes may be as long as the horns themselves. At least one or two pairs of adjacent processes are joined at their base forming a single bifurcate process with one termination inflected toward the apex, the other towards the antapex. Distal extremities of processes and all horns are solid up to a length of about 10 µm. Sulcus represented by a broad shallow depression restricted to the hypocyst; a flagellar scar is present. Archeopyle is large and represents the 2a plate, the operculum being adnate along its right lateral margin. Based on Head et al. (this issue).
Dimensions. Maximum length including horns 74 (85.5) 99 µm (Head et al., this issue).
Remarks. The cysts withstand palynological treatment (Head et al., this issue).
Biological affinity. Subfamily Protoperidinioideae according to Head et al. (this issue).
Stratigraphic range. Upper Pleistocene to modern sediments of the eastern Pacific and Upper Pleistocene to Middle Holocene sediments in the east equatorial Atlantic (Head et al., this issue).

Stelladinium reidii Bradford, 1975
Plate 16, figs. 4–6
Distinguishing characters. Cysts that are pentagonal in ambitus, often compressed dorsoventrally. Epicyst smaller than hypocyst. Five distinct horns are positioned at each of the angles on the ambitus. Supplementary horns can be present around the cingular zone. The archeopyle, when observed, is large, reflecting the 2a plate. A cingulum or sulcus may or may not be present. Wall thin, single layered, with a smooth to scabrate ornamentation. Based on Bradford (1975).
Dimensions. Cyst length 60–104 µm, width 65–103 µm (Bradford, 1975).
Remarks. The cysts withstand palynological treatment (Bradford, 1975). The difference between *Stelladinium robustum* Zonneveld, 1997 and *Stelladinium reidii* is unclear and needs further study.
Biological affinity. Initially equated with *Protoperidinium stellatum* by Bradford (1975, as *Peridinium stellatum*), the thecal equivalence is now considered unknown (Head et al., this issue).
Stratigraphic range. Upper Oligocene to Lower Miocene of Italy (Zevenboom, 1996), Lower Miocene offshore Australia (McMinn, 1993), upper Quaternary of the South China Sea (He and Sun, 1991), and modern sediments from the Persian Gulf (Bradford, 1975), Australia (Bint, 1988) and Kabira Bay, Okinawa, Japan (this study).

Genus *Trinovantedinium* Reid, 1977 emend. de Verteuil and Norris, 1992
Comments. A cyst-defined genus.

Trinovantedinium pallidifulvum Matsuoka, 1987
Plate 16, figs. 7–9
Distinguishing characters. Cysts pentagonal and light brown in color, with a thickened apical horn and two thickened antapical horns. The surface is smooth, bearing numerous penitabular and intratabular, short, solid, erect and non-branching processes with acuminate tips. The dorsal surface of the hypotheca may be striated. The archeopyle is stenodeltaform linteloid, angular and saphopylic. Based on Mertens et al. (2017).
Dimensions. Cyst length 49.9–62.8 µm, width 49.8–63.3 µm, distance between the tips of the antapical horns 20.6–22.5 µm, width of cingulum 4.8–6.5 µm, process length 1.4–2.8 µm.
Remarks. The cysts withstand palynological preparation (Mertens et al., 2017).
Biological affinity. *Protoperidinium louisianense* according to Mertens et al. (2017).

Stratigraphic range. Middle Miocene (de Verteuil and Norris, 1992, as undefined protoperidiniacean species) to modern sediments from France, the U.K., the Kattegat, Brazil, Gulf of Mexico, Saanich Inlet, B.C., Canada, Japan, China and Malaysia (Mertens et al., 2017).

Genus *Votadinium* Reid, 1977 emend. Gurdebeke et al., 2019
Comments. A cyst-defined genus differing from *Lejeunecysta* inter alia in the absence of a cingulum.

Votadinium concavum Gurdebeke, Mertens, Matsuoka, Gu and Louwye *in* Gurdebeke et al., 2019
Plate 16, figs. 10–12
Distinguishing characters. Broad cysts with concave outline on both epi- and hypocyst and shallow antapical concavity. Cyst wall smooth and pale brown. Archeopyle seems partly to involve the apex. Based on Gurdebeke et al. (2019).
Dimensions. Length 65–85 µm, width 65–85 µm, with an average length/width ratio of 0.96 (Gurdebeke et al., 2019).
Remarks. This species differs from *V. calvum* in being broader and having a less rounded and more concave outline (Gurdebeke et al., 2019). It has not yet been shown to withstand palynological treatment.
Biological affinity. Unknown; cyst-based genetic sequences show that it belongs to the Oceanica clade of the genus *Protoperidinium* (Gurdebeke et al., 2019).
Stratigraphic range. Modern sediments from the southeast coast of Iran (Attaran-Fariman et al., 2011, as *Protoperidinium* sp.) and East China Sea, Yellow Sea and Bohai Sea (Gurdebeke et al., 2019).

Votadinium elongatum He and Sun, 1991
Plate 17, figs. 1–3
Distinguishing characters. Elongate peridinioid cysts, compressed dorsoventrally with cingular area rounded. Epicyst bearing a conspicuous apical horn, cylindrical to conical. Hypocyst extending into two blunt antapical horns of approximately equal size, forming U-shaped antapical concavity. Wall thin, single-layered or with two layers closely appressed, light brown to pale yellow in color, surface smooth or with several secondary folds. Cingulum sometimes faintly expressed or marked, on the type specimen, by a transverse equatorial fold. Sulcus deep, restricted to hypocyst and broader posteriorly. Archeopyle, when present, intercalary, subcircular in outline, formed by loss of large intercalary plate 2a. Operculum free. Based on He and Sun (1991).
Dimensions. Length 70–77 µm, width 40–49 µm, apical horn length 6–10 µm, antapical horns 11–14 µm and 16 µm long, respectively (He and Sun, 1991).
Remarks. This cyst withstands palynological treatment (He and Sun, 1991).
Biological affinity. Unknown.
Stratigraphic range. Modern sediments from the South China Sea (He and Sun, 1991; Kawamura, 2004), the west coast of India (Prasad et al., 2007), and Woods Hole (Massachusetts, USA) (Wall, 1965).

Votadinium nanhaiense He and Sun, 1991
Plate 17, figs. 4–6
Distinguishing characters. Elongate peridinioid cysts, always with shoulders, compressed dorsoventrally, equatorial area prominently bulging outwards. Epicyst and hypocyst of approximately equal size. Epicyst bell-shaped with a triangular apical horn, blunt at tip. Hypocyst trapezoidal, with a gently arc-shaped antapical margin and two strongly divergent antapical horns of nearly equal size and blunt distally. Autophragm pale yellow in color, surface smooth or folded. Both cingulum and sulcus faint or absent. Archeopyle very large, intercalary, rounded six-sided or subcircular in outline, and situated in the mid-dorsal surface just below apex. Operculum free. Based on He and Sun (1991).
Dimensions. Length 65–75.8 µm, width 49–53.5 µm, apical horn length 9–11 µm, antapical horn length 6.7–11 µm (He and Sun, 1991).
Remarks. This cyst withstands palynological treatment (He and Sun, 1991).
Biological affinity. Unknown.

Stratigraphic range. Holocene including modern sediments from the South China Sea (He and Sun, 1991; Gurdebeke et al., 2019), the Arabian Sea (Jurkschat, 2003), and off the coast of India (Narale et al., 2013).

Votadinium pontifossatum Gurdebeke, Mertens, Pospelova, Matsuoka, Li and Louwye *in* Gurdebeke et al., 2019
Plate 17, figs. 7–9
Distinguishing characters. Brownish cysts with a dorsoventrally compressed pentagonal ambitus. The length is greater than the width (ratio 1.18, n=9). The epicyst has straight or slightly convex sides with a pronounced apical horn. The antapical concavity is deep and U-shaped and the antapical horns are elongated. The ornamentation consists of small rod-like elements in circular depressions, covering the entire cyst including the operculum. Archeopyle saphopylic and pentagonal, though occasionally the entire apical part (the horn) can be missing. The cingular area is sometimes devoid of ornamentation. Based on Gurdebeke et al. (2019).
Dimensions. Cyst length 65–90 µm, width 63–80 µm, length-to-width ratio 1.19–1.39 (Sarai et al., 2013).
Remarks. This cyst withstands palynological treatment (Price and Pospelova, 2011, as noted in Gurdebeke et al., 2019).
Biological affinity. *Protoperidinium paraoblongum* according to Sarai et al. (2013).
Stratigraphic range. Holocene, surface and trap sediments off Vancouver Island in Canada, as well as modern sediments from Omura Bay in Japan, Fangchenggang Port (South China Sea), and coastal sediment from Europe (U.K. and northern Germany) (Gurdebeke et al., 2019).

Votadinium psilodora (Benedek, 1972) Gurdebeke et al., 2019
Plate 17, figs. 10–12
Distinguishing characters. Peridinioid, light brown, dorsoventrally compressed cysts. The length is greater than the width (ratio=1.18, n=9). The epicyst is cone-shaped and ends in a broad rounded apical horn. The hypocyst consists of two broadly rounded antapical horns. Archeopyle trapezoid, saphopylic, corresponding to intercalary plate 2a. No trace of the cingulum. Based on Benedek (1972) and Gurdebeke et al. (2019).
Dimensions. Length 90–96 µm, width 75–78 µm (Benedek, 1972).
Remarks. This cyst withstands palynological treatment (Benedek, 1972). *Votadinium psilodora* differs from *Votadinium reidii* in having a more rounded outline and (ant)apical horns, and from *V. pontifossatum* by the absence of pontifossate ornamentation. *V. psilodora* is also distinguished from *V. calvum*, *V. spinosum*, *V. rhomboideum* and the cyst of *P. venustum* by the dorsal position of the archeopyle.
Biological affinity. Unknown.
Stratigraphic range. Mid-Oligocene deposits from Tönisbergen (NW Germany; Benedek, 1972), Pliocene deposits from Belgium (Louwye et al., 2004) and modern sediments from Akkeshi Bay, Japan (Matsuoka, 1987, 1992). Williams and Bujak (1977, p. 30, no fig.) reported *L. psilodora* as having its highest occurrence in their "*Epicephalopyxis indentata* assemblage," which ranges into the Lower Miocene.

Votadinium reidii Gurdebeke, Mertens, Pospelova, Matsuoka, Gribble and Louwye *in* Gurdebeke et al., 2019
Plate 18, 1–3
Distinguishing characters. Brownish elongated cyst with smooth wall. Outline with straight edges, especially on the left side of the cyst; right cyst variably more rounded. Apical horn variable, ranging from long and narrow to small and rounded. Antapical horns ranging from elongated to well-rounded; right antapical horn usually longer than the left. Sulcal area with flagellar scar. Intercalary archeopyle hexagonal in dorsal position, not involving apex. Based on Gurdebeke et al. (2019).
Dimensions. Cyst length 68–95 mm, width 48–68 mm (Gribble et al., 2009).

Remarks. This cyst withstands palynological treatment (Pospelova et al., 2005, mentioned in Gurdebeke et al., 2019).
Biological affinity. *Protoperidinium steidingerae* according to Gurdebeke et al. (2019).
Stratigraphic range. Modern sediments from Vineyard Sound (Massachusetts, USA) and New England, U.S.A. (Gribble et al., 2009; Gurdebeke et al., 2019).

Votadinium rhomboideum Gurdebeke, Mertens, Pospelova, Matsuoka, Li and Louwye *in* Gurdebeke et al., 2019
Plate 18, figs. 4–6
Distinguishing characters. Brownish cysts, rhomboidal in outline in ventral or dorsal view, length and width comparable. Sides of epi- and hypocyst are straight or slightly concave, conferring an angular outline. Cyst wall granular to smooth. Antapical horns rounded and generally symmetrical, sometimes right horn slightly broader. Sulcal area incised and bears flagellar scar. Antapical concavity deeply incised and U-shaped. Archeopyle (type IA of Evitt, 1985) large, trapezoidal, saphopylic and involving the apex. Based on Gurdebeke et al. (2019).
Dimensions. Cyst length 61–84 μm, width 59–80 μm, length-to-width ratio: 0.88–1.05 (Sarai et al., 2013).
Remarks. This cyst withstands palynological treatment (e.g., Pospelova et al., 2010, as noted in Gurdebeke et al., 2019). *V. rhomboideum* differs from *V. calvum* and *V. spinosum* in having a higher length/width ratio and straight outlines for the epi- and hypocyst. It lacks pronounced ornamentation, which distinguishes it from *V. spinosum* and *V. pontifossatum*, and it differs from *V. pontifossatum* and *V. reidii* in having the apex involved in the operculum. It can be distinguished from *V. nanhaiense* and *V. elongatum* by the position of the archeopyle and general outline. *V. concavum* has outlines of the epi- and hypocyst that are concave rather than straight.
Biological affinity. *Protoperidinium quadrioblongum* according to Sarai et al. (2013).
Stratigraphic range. Modern sediments worldwide (Gurdebeke et al., 2019).

Subfamily uncertain

Genus *Echinidinium* Zonneveld, 1997 ex Head et al., 2001
Comments. A cyst-defined genus.

Echinidinium aculeatum Zonneveld, 1997 ex Mertens et al., here
Plate 18, figs. 7–9
Holotype. Zonneveld, 1997, p. 328; plate III, figs. 1–3. MST-8-B6$_2$, England Finder reference O43.
Repository. Collection of Fachbereich-5 Geowissenschaften, Universität Bremen, Germany.
Type locality. Offshore Somalia, Arabian Sea.
Etymology. With reference to its aculeate process tips.
Diagnosis. Cysts with spheroidal, brown, thin-walled central body bearing randomly distributed hollow, smooth-walled processes. Between the processes isolated granules can be present. Processes taper distally to aculeate distal tips. Some aculeae may have minute bifurcations. Process bases are (sub)spherical. The theropylic archeopyle consists of a straight split. No other tabulation is reflected.
Dimensions. Central body diameter 16–26 μm, process length 6–8 μm, process basal diameter 1.5–2.5 μm (Zonneveld, 1997).
Remarks. *Echinidinium aculeatum* was not validly published in Zonneveld (1997) because its holotype was collected from a sediment trap sample (such samples have no stratigraphic relations and the contained cysts cannot therefore be treated nomenclaturally as fossils), and Latin diagnoses were not provided (Head, 2003). It is validated here, a Latin diagnosis no longer being necessary. The cysts withstand palynological treatment (Zonneveld, 1997).
Biological affinity. Unknown.

Stratigraphic range. Lower Pleistocene of the northern North Sea (Head et al., 2004) to modern sediments from the Arabian Sea, Japan, the Pacific, SW Atlantic, Brazil, Mediterranean and West African coast (Zonneveld et al., 2013)), the Hudson Bay (Heikkilä et al., 2014) and the Cariaco Basin (Bringué et al., 2019).

Echinidinium bispiniformum Zonneveld, 1997 ex Head, 2003
Plate 18, figs. 10–12
Distinguishing characters. Cysts with brown wall and spherical central body with a smooth surface bearing randomly distributed process of two types. The first is large, hollow, transparent and bulbous in outline. It is formed by separation of the luxuria and pedium. This type of process is flexible and can have fine solid spinules at the closed distal ends. Process bases are subcircular to ovoidal with a diameter of about 30% of the length. The second process type is small, solid, acuminate and scattered randomly between the large processes. These processes are flexuous, pigmented, smooth, have (sub)circular bases, and are sharply pointed at their distal ends. No tabulation is reflected except for the theropylic archeopyle which consists of a split along several sutures. Based on Zonneveld (1997).
Dimensions. Central body diameter 39–48 μm, length of large processes 4–12 μm, base of large processes 2–6 μm, length of small processes 2 μm (Zonneveld, 1997).
Remarks. The cysts withstand palynological treatment (Zonneveld, 1997).
Biological affinity. Unknown.
Stratigraphic range. Upper Pleistocene to modern sediment from the Arabian Sea (Zonneveld, 1996; Zonneveld et al., 1997).

Echinidinium delicatum Zonneveld, 1997 ex Head, 2003
Plate 19, figs. 1–3
Distinguishing characters. Cysts pale brown with spherical central body. Surface smooth bearing numerous more or less regularly distributed rigid, hollow, acuminate processes. The processes have (sub) circular bases. The theropylic archeopyle consists of a split along one or two sutures. Based on Zonneveld (1997).
Dimensions. Central body diameter 17–25 μm; process length 2–4 μm.
Remarks. The cysts withstand palynological treatment (Zonneveld, 1997).
Biological affinity. Unknown.
Stratigraphic range. Upper Pleistocene of the Arabian Sea (Zonneveld, 1997) to modern sediments from the Arabian Sea, West African coast, Brazil, Japan, northwestern Pacific and southwest Africa (Zonneveld et al., 2013).

Echinidinium granulatum Zonneveld, 1997 ex Head et al., 2001
Plate 19, figs. 4–6
Distinguishing characters. Brown cysts with spherical central body bearing numerous randomly distributed processes. The central body surface is granular. The hollow processes may bear small solid spinules at the distal ends of the processes. The processes are acuminate with closed distal ends. The broad process bases are (sub)circular to ellipsoid. Some larger processes may have longitudinal striations extending from the base. The theropylic archeopyle consists of a single split along one or two sutures. Based mostly on Zonneveld (1997).
Dimensions. Central body diameter 26–46 μm, process length 5–11 μm, diameter of process base 1–5.5 μm (Zonneveld, 1997).
Remarks. The cysts withstand palynological treatment (Zonneveld, 1997).
Biological affinity. Unknown.
Stratigraphic range. Upper Quaternary of the California margin (Pospelova et al., 2015) to modern sediments from the northwest Pacific, northeast and southeast Atlantic, South Africa, Mediterranean, and Arabian Sea (Zonneveld et al., 2013).

Echinidinium transparantum Zonneveld, 1997 ex Mertens et al., here
Plate 19, figs. 7–9
Holotype. Zonneveld, 1997, p. 329; plate III, figs. 6–8. Single Grain ARZE 2. Sample MST-8-B6.
Repository. Collection of Fachbereich-5 Geowissenschaften, Universität Bremen, Germany.
Type locality. Offshore Somalia, Arabian Sea.
Etymology. In reference to the transparent processes on this species.
Diagnosis. Small cysts with brown spherical central body bearing randomly distributed solid, transparent, acuminate processes with smooth shafts. Distal ends of processes are sharply pointed. The outline of the process bases is (sub)circular to irregularly rectangular. The central body wall is thin (less than 0.3 μm) and has an almost smooth surface, with faint, irregular granulation just visible under interference contrast microscopy. Occasional scattered granules (0.5 μm or less) and spinules are also present. The theropylic archeopyle consists of a split, probably along a single suture. No other tabulation is reflected.
Dimensions. Central body diameter 22–36 μm; process length 5–14 μm; process base 1.5–2.5 μm (Zonneveld, 1997). Central body dimensions for the holotype are 25 μm × 25 μm (not 28.4 μm as stated in Zonneveld, 1997), and 33 μm × 34 μm for the paratype (Head, 2003).
Remarks. *Echinidinium transparantum* was not validly published in Zonneveld (1997) because its holotype was collected from a sediment trap sample (such samples have no stratigraphic relations and the contained cysts cannot therefore be treated nomenclaturally as fossils), and Latin diagnoses were not provided (Head, 2003). It is validated here; a Latin diagnosis no longer being necessary. This species differs from *Echinidinium zonneveldiae* and from cysts of *Niea acanthocysta* in its smaller size and relatively longer processes. The cysts withstand palynological treatment (Zonneveld, 1997).
Biological affinity. Unknown.
Stratigraphic range. Upper Pleistocene of the Arabian Sea (Zonneveld, 1996; Zonneveld et al., 1997) to modern sediments from the Mediterranean, South Africa, Brazil, West Africa, southeast Atlantic, northeast Atlantic, Arabian Sea and Australia (Zonneveld et al., 2013).

Echinidinium zonneveldiae Head, 2003
Plate 19, figs. 10–12
Distinguishing characters. A species with light- to medium-brown spherical central body; and a thin, smooth to ornamented wall bearing solid processes that taper to fine points. Processes are less strongly colored than the central body, and are circular in transverse cross-section for most of their length, but at least some become irregularly rectangular at base; shafts are smooth. The archeopyle is theropylic, forming a long straight split. Based on Head (2003).
Dimensions. Central body diameter 35.5–51.0 μm, process length 5.0–10.0 μm (Head, 2003).
Remarks. Head (2002) remarks that this species differs from all others of the genus, with the exception of *Echinidinium transparantum* above, in the presence of solid tapering processes that arise from irregularly rectangular process bases. The cysts withstand palynological treatment (Head, 2003).
Biological affinity. Unknown.
Stratigraphic range. Upper Pleistocene (Last Interglacial) from the Baltic Sea (Head, 2003) to modern sediments from the Black Sea (Mudie et al., 2017).

Acknowledgements

It is a pleasure to thank Chris Bolch for sharing images of the cyst of *Gymnodinium trapeziforme*, Karin Zonneveld and Chris Reid for loaning their holotypes for photography, Hyeon Shin and Zhun Li for providing images of cysts of *Cochlodinium polykrikoides*, and Thomas Verleye for providing images of *Selenopemphix undulata* and loaning his slides from the Black Sea for photography, Leen Degezelle kindly helped with the digital drawings. H. Gu was supported by the National Natural Science Foundation of China (41676117). MJH and VP acknowledge support from their respective Natural Sciences and

Engineering Research Council of Canada Discovery Grants. Two anonymous reviewers are acknowledged for their helpful remarks.

Plate captions

Plate 1. 1–6. Cysts of *Barrufeta resplendens* (from modern sediment, northern Gulf of Mexico; images by KNM). 1. Living cyst with red accumulation body. 2–4. Hatched cyst showing hollow processes connected by low crests and tremic archeopyle. 5–6. Scanning electron micrograph of cyst with a focus on process structure. 7–9. Cysts of *Gymnodinium catenatum* (from modern sediment, Xiamen, East China Sea; images by HG). 7. Hatched cyst with cell still inside, showing bright red accumulation body. 8. Hatched cyst with a focus on several rows of vesicles in cinculum. 9. Scanning electron micrograph. 10–12. Cysts of *Gymnodinium inusitatum* (from modern sediment, Lianyungang, Yellow Sea; images by HG). 10. Living cyst with large and irregular granules. 11. Hatched cyst with irregular folds. 12. SEM of cyst with irregular folds. All scale bars = 10 μm.

Plate 2. 1–3. Cysts of *Gymnodinium microreticulatum* (from modern sediment, Lianyungang, Yellow Sea; images by HG). 1. Living cyst with colorless granules. 2. SEM of spherical cyst. 3. SEM of hatched cyst. 4–6. Cysts of *Gymnodinium nolleri*. 4. Specimen from modern sediment, Black Sea (GC27-0–1 cm). 5–6. Two specimens from Izmir Bay, Turkey, St. 23 (images by KNM). 7–9. Cyst of *Gymnodinium trapeziforme* from modern sediment near Pasabandar on the southeast coast of Iran, 7–8. Cyst showing trapezoidal shape. 9. SEM showing flagellar pore (fp), acrobase (g), cingular margins (c1 and c2), sulcus (s) (images by Gilan Attaran-Fariman and Christopher Bolch). 10–12. Cyst of *Margalefidinium polykrikoides* – East Asia ribotype (from modern sediment, Tongyeong coastal area, Korea; images by Zhun Li and Hyeon Ho Shin). All scale bars = 10 μm.

Plate 3. 1–3. Cysts of *Polykrikos hartmannii* (from modern sediment, Omura Bay, Japan; images by KNM). 1–2. Living cyst with colorless granules and red body. 3. Hatched cyst showing distinct surface ornamentation. 4–6. Cyst of *Polykrikos* sp. sensu Fukuyo, 1982, plate II, figs. 1–4, high to low focus of specimen (from modern sediment, Saanich Inlet, B.C., Canada, EXP61A; images by KNM). All scale bars = 10 μm.

Plate 4. 1–3. Cyst of *Boreadinium breve* (from modern sediment, Lianyungang, Yellow Sea; images by HG). 1–2. Living cysts with colorless granules. 3. Hatched cyst displaying archeopyle. 4–6. Cyst of *Diplopelta globula* (from modern sediment, Fangchenggang, South China Sea; images by HG). 4. Living cyst with colorless granules. 5–6. Hatched cysts displaying archeopyle. 7–9. Hatched cyst of *Diplopelta symmetrica* showing theropylic archeopyle and hairy surface ornamentation (from modern sediment, Bantry, Ireland; images by KNM). 10–12. Single specimen of hatched cyst of *Diplopsalis lenticula* displaying theropylic archeopyle (from modern sediment, German Wadden Sea; images by KNM). All scale bars = 10 μm.

Plate 5. 1–3. Hatched cysts of *Diplopsalopsis latipeltata* (from modern sediment, San Pedro Harbor, California, U.S.A.; images by KNM). 4–6. Cyst of *Diplopsalopsis ovata* (from modern sediment off Sasebo, Japan; images by KNM). 7–9. *Dubridinium caperatum* (from modern sediment of Izmir Bay, Turkey, images by KNM). 7. LM micrographs. 8–9. SEM micrograph. 10–12. *Dubridinium cassiculum* (holotype 88K3 from modern sediment off Lytham St. Annes, England; images by PG). All scale bars = 10 μm.

Plate 6. 1–3. *Dubridinium cavatum* from modern sediment, Caernavon, Wales, UK, high to mid-focus of same specimen (images by KNM). 4–6. Different orientations of hatched specimen of *Dubridinium ulsterum* showing verrucate ornamentation (from modern sediment, Bantry, Ireland; images by KNM). 7–9. Cysts of *Huia caspica* (specimens from modern sediment, Fuzhou, East China Sea; images by HG). 7.

Living cyst with greenish granules. 8–9. Hatched cyst displaying archeopyle. 10–12. Cysts of *Lebouraia pusilla*. 10. Living cyst with greenish granules (from modern sediment, Fangchenggang, South China Sea; images by HG). 11–12. Hatched cyst (from modern sediment, Bourcefranc, Charente-Maritime, France; images by KNM). All scale bars = 10 µm.

Plate 7. 1–3. Cysts of *Niea acanthocysta* (from modern sediment, Omura Bay, Japan). 1–2. LM images (by KNM). 3. SEM image (by Marianne Ellegaard). 4–6. Cysts of *Niea chinensis* (from modern sediment, Fangchenggang, South China Sea; images by HG). 4. Living cyst with colorless granules. 5–6. Hatched cysts displaying archeopyle (LM and SEM). 7–9. Cysts of *Niea torta* (from modern sediment, Qingdao, Yellow Sea; images by HG). 10–12. Cyst of *Oblea rotunda*. 10. Living cyst with greenish granules (from modern sediment, Ninde, East China Sea; image by HG). 11–12. Hatched cysts showing archeopyle (from modern sediment off Sasebo, Japan; images by KNM). All scale bars = 10 µm.

Plate 8. 1–3. Cysts of *Qia lebouriae*. 1–2. High to mid-focus of living specimen (from modern sediment, Omura Bay, Japan; images by KNM). 3. Mid focus of hatched cyst (from modern sediment, Fangchenggang, South China Sea; images by HG). 4–6. Cyst of *Archaeperidinium bailongense* showing different orientations of same specimen, archeopyle is visible in 6 (from modern sediment, Bailong, Fangchenggang, Guangxi province, China; images by KNM). 7–9. Cysts of *Archaeperidinium constrictum* (from modern sediment, Omura Bay, Japan; images by KNM). 7–8. Living cysts with transparent granules. 9. Empty cyst displaying the wide bases of the many processes. 10–12. Cysts of *Archaeperidinium minutum* sensu stricto (images by KNM). 10–11. Specimen from modern sediment, Bay of Vilaine, France. 12. SEM of specimen from modern sediment, Vie Estuary, France. All scale bars = 10 µm.

Plate 9. 1–3. Cysts of *Archaeperidinium minutum* sensu Wall and Dale, 1968 (images by KNM). 1–2. Specimen from modern sediment, Baie de Vilaine, France. 3. SEM of specimen from modern sediment, Vie Estuary, France. 4–6. Cysts of *Archaeperidinium monospinum* (images by KNM). 4–5. Specimen displaying archeopyle and the two types of processes (from modern sediment, Baie de Vilaine, France). 6. SEM of specimen from modern sediment, Vie Estuary, France. 7–9. Cysts of *Archaeperidinium saanichi* displaying archeopyle (from modern sediment, Saanich Inlet, UVic08-005; images by KNM). 10–12. *Brigantedinium asymmetricum*. 10–11. High to low focus of specimen from modern sediment, Lake Saroma, Japan. 12. SEM of specimen from modern sediment, Lake Saroma, Japan showing microgranular wall surface (images by KNM). All scale bars = 10 µm.

Plate 10. 1–3. *Brigantedinium auranteum* from modern sediment, Patricia Bay, Saanich Inlet, B.C., Canada (images by PG). 4,6. *Brigantedinium majusculum* from modern sediment, Izmir Bay, Turkey (images by KNM). 5. *Brigantedinium majusculum,* specimen from modern sediment from Tongyeong coastal area, Korea (image by Zhun Li and Hyeon Ho Shin). 4. High to mid-focus showing archeopyle. 6. SEM image showing smooth wall. 7–9. *Cristadinium striatiserratum* (both specimens from upper Quaternary sediment, Cariaco Basin, Venezuela; Mertens et al., 2009; images by KNM). 7–8. High to low focus. 9. Dorsal view of the epicyst. 10–12. *Islandinium pacificum* (images by KNM). 10–11. Holotype from modern sediment, Saanich Inlet, B.C., Canada, UVic 2009-661-1 (images by KNM). 12. SEM from modern sediment, Saanich Inlet, Station 2 of Mertens et al. (2012b) (image by KNM). All scale bars = 10 µm.

Plate 11. 1–2. High to low focus of *Leipokatium invisitatum* (from modern sediment, South China Sea, UVic 2017-53; images by ZL). 3–6. Holotype of *Lejeunecysta*? *epidoma* from modern sediment Akkeshi Bay, Hokkaido, Japan (images by KNM). 7–9. *Lejeunecysta marieae*. 7. Specimen from upper Quaternary sediment, Cariaco Basin, Venezuela (Mertens et al., 2009; image by KNM). 8–9. High to low focus of specimen from modern sediment, Nova Scotia, Canada (2219-1, images by KNM). 10–12. Cysts of *Protoperidinium abei* var. *rotundata*. 10. Living specimen from modern sediment, Lianyungang,

Yellow Sea (image by HG). 11. High focus of specimen from modern sediment, Lianyungang, Yellow Sea (image by HG). 12. SEM of specimens from modern sediment, Wenzhou (East China Sea) (image by KNM and ZL). All scale bars = 10 μm.

Plate 12. 1–3. Cyst of *Protoperidinium biconicum* (from modern sediment, Fangchenggang, South China Sea; images by HG). 1. Apical view. 2. Ventral view. 3. Dorsal view showing operculum still in place. 4–6. Cysts of *Protoperidinium denticulatum* (from modern sediment, Byfjorden, Norway; images by KNM). 4. High focus of specimen displaying distinct archeopyle. 5–6. High to mid focus of specimen. 7–9. Cysts of *Protoperidinium excentricum* (images by KNM). 7–8. Different orientations of specimen from modern sediment, Central Saanich Inlet, B.C., Canada. 9. Hatched specimen from modern sediment, Patricia Bay, Vancouver Island, B.C., Canada. 10–12. High to mid focus of cyst of *Protoperidinium fukuyoi* (from modern sediment, Brentwood Bay, Vancouver Island, B.C., Canada; images by YT). All scale bars = 10 μm.

Plate 13. 1–3. Cyst of *Protoperidinium fuzhouense*, hatched specimen (from modern sediment, Fuzhou, East China Sea; images by HG). 4–5. Cysts of *Protoperidinium humile*, hatched specimen (from modern sediment, Fangchenggang, South China Sea; images by HG). 6–9. Cysts of *Protoperidinium latissimum*, specimens (6,9 from modern sediment, Omura Bay, Japan; images by KNM; 7,8 from modern sediment from south Korean coastal area; images by ZL and HHS). 10–12. High to low focus of cyst of *Protoperidinium lewisiae*, living cyst (from modern sediment, Qingdao, China; images by KNM). All scale bars = 10 μm.

Plate 14. 1–3. 1–3. Cyst of *Protoperidinium parthenopes* (from modern sediment, Sea of Okhotsk; images by KNM). 4–6. Cyst of *Protoperidinium punctulatum*, high focus of different orientations of hatched specimen from modern sediment, Patricia Bay, Vancouver Island, B.C., Canada. 7–9. Cyst of *Protoperidinium thorianum* (from modern sediments, Bantry, Ireland; images by KNM). 7. Living cyst with reddish granules. 8–9. High to mid focus of hatched specimen, displaying archeopyle. 10–12. Cyst of *Protoperidinium thulesense*. Hatched specimen showing theropylic archeopyle (from modern sediment, Sasebo, Japan; images by KNM). All scale bars = 10 μm.

Plate 15. 1–3. Cysts of *Protoperidinium tricingulatum* (images by KNM). 1. Living cyst from modern sediment from Lake Saroma, Hokkaido, Japan. 2–3. Hatched specimen from modern sediment, Lake Notoro, Hokkaido, Japan. 4–6. *Selenopemphix tholus*, single specimen from modern sediment, Sasebo, Japan; images by KNM). 4. High focus of ventral side. 5. Mid focus. 6. Mid focus showing cingular cross-section. 7–9. *Selenopemphix undulata* (images by Thomas Verleye). 7–8. Holotype from modern sediment, SE Pacific, offshore central-south Chile (41°S), high focus of antapical view and low focus of apical view. 9. Other specimen from SE Pacific showing ventral view. 10–12. *Stelladinium abei*, high to low focus of holotype (images by KNM) from modern sediment, Senzaki Bay, Japan. All scale bars = 10 μm.

Plate 16. 1–3. *Stelladinium bifidum*, high to mid-focus of holotype, dorsal view (from modern sediments, La Paz Bay, Gulf of California; images by MJH). 4–6. *Stelladinium reidii*, different orientations of single specimen (from modern sediment, Kabira Bay, Okinawa, Japan; images by KNM). 4. Dorsal view, showing archeopyle. 5. Ventral view. 6. Dorso-lateral view. 7–9. *Trinovantedinium pallidifulvum*, single specimen (from modern sediment, Gulf of Mexico; images by KNM). 7. High focus of ventral view. 8. Mid focus. 9. Low focus of dorsal view. 10–12. *Votadinium concavum* (modern sediment, Bohai Sea, China; images by HG). 10. SEM micrograph of holotype. 11–12. LM optical sections. All scale bars = 10 μm.

Plate 17. 1–3. *Votadinium elongatum* (from modern sediment from the South China Sea; images by ZL). 4–6. *Votadinium nanhaiense* at progressively lower foci (from modern sediment, South China Sea;

images by ZL). 7–9. *Votadinium pontifossatum*, hatched specimen (from modern sediment, Patricia Bay, Vancouver Island, B.C., Canada; images by KNM). 7. Dorsal view. 8. Focus on archeopyle with operculum in place. 9. Ventral view with focus on sulcus. 10–12. *Votadinium psilodora*, holotype, mid-Oligocene of Tönisbergen (Germany), progressively lower foci (images by PG). All scale bars = 10 µm.

Plate 18. 1–3. *Votadinium reidii* from cultures based on material from Vineyard Sound, Massachussetts, U.S.A. SEM images (images by KNM). 2. Holotype. 3. Antapical view showing flagellar scar. 4–6. *Votadinium rhomboideum* (from modern sediment, Kabira Bay, Okinawa, Japan; images by KNM). 4–5. High to mid focus of dorsal view. 6. Mid focus of apical view. 7–9. *Echinidinium aculeatum*. 7–8. High to lower focus of specimen from modern sediment, Saanich Inlet (images by KNM). 9. SEM of specimen from modern sediment, Saanich Inlet (EXP61A) (image by PG and KNM). 10–12. *Echinidinium bispiniformum*, high to low focus of holotype (from modern sediment, offshore Yemen, Arabian Sea; images by KNM). All scale bars = 10 µm.

Plate 19. 1–3. *Echinidinium delicatum*, high to low focus of holotype (from modern sediment, offshore Pakistan, Arabian Sea; images by KNM). 4–6. *Echinidinium granulatum*, high to low focus. 7–9. *Echinidinium transparatum*, high to mid focus of holotype (from modern sediment, offshore Somalia, Arabian Sea; images by KNM). 10–12. *Echinidinium zonneveldiae*, high to mid focus of specimen from modern sediment, Black Sea, core GeoB7625-2 (464 cm, Holocene) (images by KNM).

Figure captions.

Figure 1. Schematic drawings of round brown cysts with saphopylic archeopyle, all drawn to scale. A. Cyst of *Diplopsalopsis ovata*. B. *Brigantedinium auranteum*. C. *Brigantedinium asymmetricum*. D. Cyst of *Protoperidinium avellana*. E. Cyst of *Protoperidinium abei* var. *rotundata*. F. Cyst of *Protoperidinium thorianum*. G. Cyst of *Protoperidinium denticulatum*. H. Cyst of *Protoperidinium punctulatum*. I. *Brigantedinium simplex*. J. *Brigantedinium majusculum*. Scale bar = 10 µm.

Figure 2. Schematic drawings of round brown cysts with theropylic archeopyle, all drawn to scale. A. Cyst of *Oblea rotunda*. B. *Lebouraia pusilla*. C. Cyst of *Huia caspica*. D. Cyst of *Protoperidinium thulesense*. E. Cyst of *Boreadinium breve*. F. Cyst of *Diplopsalopsis latipeltata*. G. Cyst of *Diplopsalis lenticula*. H. Cyst of *Qia lebouriae*. I. Cyst of *Protoperidinium fuzhouense*. J. Cyst of *Niea torta*. K. Cyst of *Niea chinensis*. L. Cyst of *Diplopelta globula*. Scale bar = 10 µm.

References

Abé, T.H., 1936. Report of the biological survey of Mutsu Bay. 29. Notes on the protozoan fauna of Mutsu Bay. II. Genus *Peridinium*; subgenus *Archaeperidinium*. Scientific Reports of Tohoku University, Series 4, Biology 10, 639–686.

Abé T.H., 1941. Studies on the Protozoan Fauna of Shimoda Bay. The *Diplopsalis* group. Records of Ocean Works in Japan 12, 121–144.

Abé, T.H., 1981. Studies on the Family Peridinidae. An Unfinished Monograph of the Armored Dinoflagellata. Tokyo, Academia Scientific Book, 409 pp.

Akselman, R., 1987. Quistes planctonicos de dinoficeas en areas de plataforma del Atlantico Sudoccidental. I. Reporte taxonomico de la familia Peridiniaceae Ehrenberg. Boletim do Instituto Oceanográfico do Sao Paulo 35, 17–32.

Amorim, A., Dale, B., 2006. Historical cyst record as evidence for the recent introduction of the dinoflagellate *Gymnodinium catenatum* in the North-Eastern Atlantic. African Journal of Marine Science 28, 193–197.

Amorim, A., Dale, B., Godinho, R., Brotas, V., 2002. *Gymnodinium catenatum*-like cysts (Dinophyceae) in recent sediments from the coast of Portugal. Phycologia 40, 572–582.

Anderson D.M., Jacobsen, D.J., Bravo, I., Wrenn, J.H., 1988. The unique, microreticulate cyst of the naked dinoflagellate *Gymnodinium catenatum*. Journal of Phycology 24, 255–262.

Apstein, C., 1909. Die Pyrocysteen der Plankton-Expedition. In: Ergebnisse der Plankton-Expedition der Humboldt-Stiftung. Bd. IV. M.c. Kiel, Lipsius and Tischer, 27 pp.

Artzner, D.G., Dörhöfer, G., 1978. Taxonomic note: *Lejeunecysta* nom. nov. pro *Lejeunia* Gerlach 1961 emend. Lentin and Williams 1976 – dinoflagellate cyst genus. Canadian Journal of Botany 56, 1381–1382.

Attaran-Fariman, G., de Salas, M.F., Negri, A.P., Bolch, C.J.S., 2007. Morphology and phylogeny of *Gymnodinium trapeziforme* sp. nov. (Dinophyceae): a new dinoflagellate from the southeast coast of Iran that forms microreticulate resting cysts. Phycologia 46, 644-656.

Attaran-Fariman, G., Khodami, S., Bolch, C.J.S., 2011. The cyst-motile relationship of three *Protoperidinium* species from south-east coast of Iran. Iranian Journal of Fisheries Science 10, 1–12.

Aydin, H., Matsuoka, K., Minareci, E., 2011. Distribution of dinoflagellate cysts in recent sediments from Izmir Bay (Aegean Sea, Eastern Mediterranean). Marine Micropaleontology 80, 44–52.

Balech, E., 1958. Plancton de la Campaña Antártica Argentina 1954-1955. Physis 21, 85–108.

Balech E., 1964. El plancton de Mar del Plata durante el período 1961–1962 (Buenos Aires, Argentina). Boletín del Instituto de Biología Marina 4, 1–49.

Balech, E., 1973. Cuarta contribucion al conocimiento del genero *Protoperidinium*. Revista del Museo Argentino de Ciencias Naturales Nueva Serie 3, 347–368.

Balech, E., 1974. El género "*Protoperidinium*" Bergh, 1881 ("*Peridinium*" Ehrenberg, 1831, partim). Revista del Museo Argentino de ciencias naturales "Bernardino Rivadavia", Hidrobiología 4(1), 1–79.

Balech E., 1979. Dinoflagellados. Campana Oceanografica Argentina <<Islas Orcadas>> 06/75. Republica Argentina, Armada Argentina Servico de Hidrografia Naval, Buenos Aires 655, 1–76.

Balech, E., 1988. Los dinoflagellados del Atlantico sudoccidental. Publicaciones Especiales del Instituto Español de Oceanografía 1, Madrid, Spain, 310 pp.

Balech E., Akselman, R., 1988. Un nuevo Diplopsaliinae (Dinoflagellatae) de Patagonia, Argentina. Physis (Buenos Aires) Sec. A 46(110), 27–30.

Balech E., Borgese, B., 1990. *Diplopsalopsis latipeltata*, una nueva especie de Dinoflagellata. Anal. Acad. Nac. Cs. Ex. Fis. Nat., Buenos Aires 42, 251–255.

Benedek, P.N., 1972. Phytoplanktonten aus dem Mittel- und Oberoligozän von Tönisberg (Niederrheingebiet). Palaeontographica Abteilung B 137, 1–71.

Bergh, R.S., 1881a. Bidrag til cilioflagellaternes naturhistorie. Forelobige meddelelser. Dansk Naturhistoriskforening i Kjobenhavn, Videnskabelige Meddelelser, Series 4(3), 60–76.

Bergh R.S., 1881b. Der Organismus der Cilioflagellaten. Eine phylogenetische Studie. Gegenbauer's Morphologisches Jahrbuch 7(2), 177–288+ pls 12–16.

Bint, A.N., 1988. Recent dinoflagellate cysts from Mermaid Sound, northwestern Australia. In: P.A. Jell and G. Playford (editors), Palynological and Palaeobotanical Studies in Honour of Basil E. Balme. Memoir of the Association of Australasian Palaeontologists 5, 329–341.

Bolch, C.J.S., Reynolds, M.J., 2002. Species resolution and global distribution of microreticulate dinoflagellate cysts. Journal of Plankton Research 24, 565–578.

Bolch, C.J.S., Negri, A., Hallegraeff, G.M., 1999. *Gymnodinium microreticulatum* sp. nov. (Dinophyceae): a naked, microreticulate cyst producing dinoflagellate, distinct from *Gymnodinium catenatum* Graham and *Gymnodinium nolleri* Ellegaard et Moestrup. Phycologia 38, 301–313.

Bradford, M.R., 1975. New dinoflagellate cyst genera from the recent sediments of the Persian Gulf. Canadian Journal of Botany 53, 3064–3074.

Bringué, M., Pospelova, V., Field, D.B. 2014. High resolution dinoflagellate cyst record of decadal variability and 20th century warming in the Santa Barbara Basin, California. Quaternary Science Reviews 105, 86–101.

Bringué, M., Pospelova, V., Tappa, E.J. and Thunell, R.C., 2019. Dinoflagellate cyst production in the Cariaco Basin: a 12 year-long sediment trap study. Progress in Oceanography 171, 175–211.

Bujak, J.P., Matsuoka, K., 1986. Taxonomic reallocation of Cenozoic dinoflagellate cysts from Japan and the Bering Sea. Palynology 10, 235–241.

Bütschli, O., 1873. Einiges über Infusorien. Archiv für Mikroskopische Anatomie 9, 657–678.

Bütschli, O., 1885. 3. Unterabtheilung (Ordnung) Dinoflagellata. In: Dr. H.G. Bronn's Klassen und Ordnungen des Thier-Reichs, wissenschaftlich dargestellt in Wort und Bild. Erster Band Protozoa. C.F. Wintersche Verlagshandlung, Leipzig und Heidelberg, p. 906–1029.

Cho, H.J., Kim, C.H., Moon, C.H., Matsuoka, K., 2003. Dinoflagellate cysts in recent sediments from the southern coastal waters of Korea. Botanica Marina 46, 332–337.

Dale, B., 1983. Dinoflagellate resting cysts: "benthic plankton". In: Fryxell, G.A. (ed.), Survival Strategies of the Algae; Cambridge, UK, Cambridge University Press, p. 69–136.

Dale, B., Montresor, M., Zingone, A., Zonneveld, K., 1993. The cyst-motile stage relationships of the dinoflagellates *Diplopelta symmetrica* and *Diplopsalopsis latipeltata*. European Journal of Phycology 28, 129–137.

Dangeard, P.A., 1927. Péridiniens nouveaux ou peu connus de la croisiére du „Sylvana". Bulletin de l'Institut Océanographique 491, 1–16.

D'Costa, P.M., Anil, A.C., Patil, J.S., Hegde, S., D'Silva, M.S., Chourasia, M., 2008. Dinoflagellates in a mesotrophic, tropical environment influenced by monsoon. Estuarine, Coastal and Shelf Science 77, 77–90.

D'Silva, M.S., Anil, A.C., D'Costa, P.M., 2011. An overview of dinoflagellate cysts in recent sediments along the west coast of India. Indian Journal of Geo-Marine Sciences 40, 697–709.

de Vernal, A., Radi, T., Zaragosi, S., Van Nieuwenhove, N., Rochon, A., Allan, E., De Schepper, S., Eynaud, F., Head, M.J., Limoges, A., Londeix, L., Marret, F., Matthiessen, J., Penaud, A., Pospelova, V., Richerol, T., 2019. Distribution of common modern dinocyst taxa in surface sediment of the Northern Hemisphere in relation to environmental parameters: the updated n=1968 database. Marine Micropaleontology, this issue.

de Verteuil, L., 1996. 27. Data report: upper Cenozoic dinoflagellate cysts from the continental slope and rise off New Jersey. In: Mountain, G.S., Miller, K.G., Blum, P., Poag, C.W., Twichell, D.C. (Eds.). Proceedings of the Ocean Drilling Program, Scientific Results 150, pp. 439–454.

de Verteuil, L., Norris, G., 1992. Miocene protoperidiniacean dinoflagellate cysts from the Maryland and Virginia coastal plain. In: Head, M.J., Wrenn, J.H. (eds.). Neogene and Quaternary Dinoflagellate Cysts and Acritarchs. American Association of Stratigraphic Palynologists Foundation, Dallas, U.S.A., p. 391–430.

Dobell, P.E.R., 1978. A study of dinoflagellate cysts from Recent sediments of British Columbia. Unpublished MSc. Thesis, University of British Columbia, Vancouver, B.C., Canada.

Dodge, J.D., 1983. Ornamentation of thecal plates in *Protoperidinium* (Dinophyceae) as seen by scanning electron microscopy. Journal of Plankton Research 5, 119–127.

Dodge, J.D., Hermes, H.B., 1981. A revision of the *Diplopsalis* group of dinoflagellates (Dinophyceae) based on material from the British Isles. Linnean Society, Botanical Journal 83, 15–26.

Dodge, J.D., Toriumi, S., 1993. A taxonomic revision of the *Diplopsalis* group (Dinophyceae). Botanica Marina 36, 137–147.

Elbrächter, M., 1993. *Kolkwitziella* Lindemann 1919 and *Preperidinium* Mangin 1913: correct generic names in the *Diplopsalis*-group (Dinophyceae). Nova Hedwigia 56, 173–178.

Ellegaard, M., Moestrup, Ø., 1999. Fine structure of the flagellar apparatus and morphological details of *Gymnodinium nolleri* sp. nov. (Dinophyceae), an unarmored dinoflagellate producing a microreticulate cyst. Phycologia 38(4), 289–300.

Ellegaard, M., Christensen, N.F., Moestrup, Ø., 1994. Dinoflagellate cysts from Recent Danish marine sediments. European Journal of Phycology 29, 183–194.

Evitt, W.R., 1985. Sporopollenin dinoflagellate cysts: their morphology and interpretation. American Association of Stratigraphic Palynologists Foundation, Dallas, Texas, i–xv + 333 p.

Fensome, R.A., Taylor, F.J.R., Norris, G., Sarjeant, W.A.S., Wharton, D.I., Williams, G.L., 1993. A classification of living and fossil dinoflagellates. Micropaleontology Special Publications 7, 1–351.

Fensome, R., Bijl, P., Grothe, A., Head, M., Sangiorgi, F., Williams, G., 2016. (2450-2451) Proposals to conserve the names *Selenopemphix* against *Margosphaera*, and *S. nephroides* against *M. velata* (Dinophyceae). Taxon 65(3), 636–637

Fukuyo, Y., 1982. Cysts of naked dinoflagellates. In: Okaichi, T. (ed.), Fundamental Studies of the Effects of the Marine Environment on the Outbreaks of Red Tides. Reports of Environmental Sciences, B 148-R14-8, Monbusho, Tokyo, pp. 205–214.

Fukuyo, Y., Kittaka, J., Hirano, R., 1977. Studies on the cysts of marine dinoflagellates – I *Protoperidinium minutum* (Kofoid) Loeblich. Bulletin of the Plankton Society of Japan 24, 11–18.

Fukuyo, Y., Sako, Y., Matsuoka, K., Imai, I., Takahashi, M., Watanabe, M., 2003. Biological character of red-tide organisms. In: Okaichi, T. (ed.), Red Tides. Terra Scientific Publishing Company, Tokyo, p. 61–153.

García-Moreiras, I., Pospelova, V., García-Gil, S., Muñoz Sobrino, C, 2018. Climatic and anthropogenic impacts on the Ría de Vigo (NW Iberia) over the last two centuries: a high-resolution dinoflagellate cyst sedimentary record. Palaeogeography, Palaeoclimatology, Palaeoecology 504, 201–218.

Godhe, A., Karunasagar, I., Karlson, B., 2000. Dinoflagellate cysts in recent marine sediments from SW India. Botanica Marina 43, 39–48.

Gómez, F., 2012. A quantitative review of the lifestyle, habitat and trophic diversity of dinoflagellates (Dinoflagellata, Alveolata). Systematics and Biodiversity 10(3), 267–275.

Gómez, F., Mindy L. Richlen, M.L., Anderson, D.M., 2017. Molecular characterization and morphology of *Cochlodinium strangulatum*, the type species of *Cochlodinium*, and *Margalefidinium* gen. nov. for *C. polykrikoides* and allied species (Gymnodiniales, Dinophyceae). Harmful Algae 63, 32–44.

Graham, H.W., 1942: Studies in the morphology, taxonomy, and ecology of the Peridiniales. In: Scientific Results of Cruise VII of the Carnegie during 1928-1929 under command of Captain J.P. Ault, Carnegie Institution of Washington, Publication, 542:v+120 p.

Gran, H.H., Braarud, T., 1935. A quantitative study of the phytoplankton in the Bay of Fundy and the Gulf of Maine (including observations on hydrography, chemistry and turbidity). Journal of the Biological Board of Canada 1, 279–467.

Gribble, K.E., Anderson, D.M., Coats, D.W., 2009. Sexual and asexual processes in *Protoperidinium steidingerae* Balech (Dinophyceae), with observations on life-history stages of *Protoperidinium depressum* (Bailey) Balech (Dinophyceae). Journal of Eukaryotic Microbiology 56, 88–103.

Gu, H., Liu, T., Vale, P., Luo, Z., 2013. Morphology, phylogeny and toxin profiles of *Gymnodinium inusitatum* sp. nov., *Gymnodinium catenatum* and *Gymnodinium microreticulatum* (Dinophyceae) from the Yellow Sea, China. Harmful Algae 28, 97–107.

Gu, H., Liu, T., Mertens, K.N., 2015b. Cyst-theca relationship and phylogenetic positions of *Protoperidinium* (Peridiniales, Dinophyceae) species of the sections *Conica* and *Tabulata*, with description of *Protoperidinium shanghaiense* sp. nov.. Phycologia 54(1), 49–66.

Gu, H., Luo, Z., Mertens, K.N., Price, A.M., Turner, R.E., Rabalais, N.N., 2015a. Cyst-motile stage relationship, morphology, ultrastructure, and molecular phylogeny of the gymnodinioid dinoflagellate

Barrufeta resplendens comb. nov., formerly known as *Gyrodinium resplendens*, isolated from the Gulf of Mexico. Journal of Phycology 51, 990–999.

Gu, H., Mertens, K.N., Liu, T., 2016. *Huia caspica* gen. & comb. nov., a dinoflagellate species that recently crossed the marine-freshwater boundary. Phycological Research 64, 251–258.

Gurdebeke, P.R., Mertens, K.N., Pospelova, V., Van Nieuwenhove, N., Louwye, S., 2019. *Islandinium pacificum*, a new dinoflagellate cyst species from late Quaternary sediment of the NE Pacific (Dinophyceae, Peridiniales). Palynology, https://doi.org/10.1080/01916122.2018.1549118.

Gurdebeke, P.R., Mertens, K.N., Pospelova, V., Matsuoka, K., Li, Z., Gribble, K.E., Gu, H., Bogus, K., Vrielinck, H., Louwye, S., 2019. Taxonomic revision, phylogeny, and cyst wall composition of the dinoflagellate cyst genus *Votadinium* Reid (Dinophyceae, Peridiniales, Protoperidiniaceae). Palynology, https://doi.org/10.1080/01916122.2019.1580627.

Haeckel, E., 1894. Systematische Phylogenie. Entwurf eines natürlichen Systems der Organismen auf Grund ihrer Stammegeschichte, I. Systematische Phylogenie der Protisten und Pflanzen. Reimer, Berlin, Germany, xv+400 pp.

Harland, R., 1977. Recent and Late Quaternary (Flandrian and Devensian) dinoflagellate cysts from marine continental shelf sediments around the British Isles. Paleontographica Abteilung B 164, 87−126.

Harland, R., Bonny, A.P., Hughes, M.J., Morigi, A.N., 1991. The Lower Pleistocene stratigraphy of the Ormesby Borehole, Norfolk, England. Geological Magazine 128(6), 647–660.

He Chengquan, Song Zhichen and Zhu Youhua, 2009. Fossil dinoflagellates of China. Nanjing Institute of Geology and Palaeontology, Chinese Academy of Sciences, Nanjing 2100089, 737 p.

He Chengquan, Sun Xuekun, 1991. 7. Dinoflagellate cysts from Quaternary sediments of Nansha, the South China Sea. In: The Multidisciplinary Oceanographic Expedition Team of Academia Sinica to the Nansha Islands (editors), Quaternary Biological Groups of the Nansha Islands and the Neighbouring Waters, p. 266–302, 520–525, Science Press, Beijing, China.

Head, M.J., 1993. Dinoflagellates, sporomorphs and other palynomorphs from the Upper Pliocene St. Erth Beds of Cornwall, southwestern England. Journal of Paleontology, Memoir 31, 1–62.

Head, M.J., 1996. Chapter 30. Modern dinoflagellate cysts and their biological affinities. In: Jansonius, J., McGregor, D.C. (eds.), Palynology: Principles and Applications. American Association of Stratigraphic Palynologists Foundation, Dallas, Texas, vol. 3, p. 1197–1248.

Head, M.J., 2003. *Echinidinium zonneveldiae* sp. nov., a dinoflagellate cyst from the late Pleistocene of the Baltic Sea, northern Europe. Journal of Micropalaeontology 21, 169–173. [Cover date 2002, issue date March 2003.]

Head, M.J., Norris, G., Mudie, P.J., 1989. New species of dinocysts and a new species of acritarch from the upper Miocene and lowermost Pliocene, ODP Leg 105, Site 646, Labrador Sea. Proceedings of the Ocean Drilling Program, Scientific Results 105, 453–466.

Head, M.J., Harland, R. and Matthiessen, J., 2001. Cold marine indicators of the late Quaternary: the new dinoflagellate cyst genus *Islandinium* and related morphotypes. Journal of Quaternary Science, 16, 621–636, pl. 1–3.

Head, M.J., Riding, J.B., Eidvin, T., Chadwick, R.A., 2004. Palynological and foraminiferal biostratigraphy of (Upper Pliocene) Nordland Group mudstones at Sleipner, northern North Sea. Marine and Petroleum Geology 21, 277–297.

Head, M.J., Fensome, R.A., Herendeen, P.S., Skog, J.E., 2016. (315–319) Proposals to amend Article 11.8 and its Examples to remove ambiguity in the sanctioning of dual nomenclature for dinoflagellates, and an emendation of Article 11.7, Example 29. Taxon 65(4): 902–903.

Head, M.J., Pospelova, V., Radi, T., Marret, F., 2019. *Stelladinium bifidum* sp. nov., a distinctive extant thermophilic heterotrophic dinoflagellate cyst from the late Quaternary of the eastern Pacific and east equatorial Atlantic oceans. Marine Micropaleontology, this issue.

Heikkilä, M., Pospelova, V., Hochheim, K.P., Kuzyk, Z.Z.A., Stern, G.A., Macdonald, R.W., Barber, D.G., 2014. Surface sediment dinoflagellate cysts from the Hudson Bay system and their relation to freshwater and nutrient cycling. Marine Micropaleontology 106, 79–109.

Hoppenrath, M., Leander, B.S., 2010. Dinoflagellate phylogeny as inferred from Heat Shock Protein 90 and ribosomal gene sequences. PLoS ONE 5(10), e13220 (12 pages).

Hoppenrath, M., Yubuki, N., Bachvaroff, T.R., Leander, B.S., 2010. Re-classification of *Pheopolykrikos hartmannii* as *Polykrikos* (Dinophyceae) based partly on the ultrastructure of complex extrusomes. European Journal of Protistology 46, 29–37.

Hulburt, E.M., 1957. The taxonomy of unarmoured Dinophyceae of shallow embayments on Cape Cod, Massachusetts. Biological Bulletin 112, 196–219.

Jiménez-Moreno, G., Head, M.J., Harzhauser, M., 2006. Early and Middle Miocene dinoflagellate cyst stratigraphy of the Central Paratethys, Central Europe. Journal of Micropalaeontology 25, 113–139.

Jörgensen, E., 1912. Bericht über die von der schwedischen Hydrographisch-Biologischen Kommission in den schwedischen Gewässern in den Jahren 1909–1910 eingesammelten Planktonproben. Svenska Hydrogrfiska-Biologiska Kommisionen, Skrifter 4, 1–20.

Jurkschat, T., 2003. Paläoproduktivitäts-Schwankungen und Veränderungen der paläozeanographischen Bedingungen im Arabischen Meer während der letzten 130.000 Jahre –rekonstruiert anhand von organischen Dinoflagellatenzysten. PhD-thesis, Hannover University.

Kawami, H., Matsuoka, K., 2009. A new cyst-theca relationship for *Protoperidinium parthenopes* Zingone & Montresor 1988 (Peridiniales, Dinophyceae). Palynology 33, 11–18.

Kawami, H., Iwataki, M., Matsuoka, K., 2006. A new diplopsalid species *Oblea acanthocysta* sp. nov. (Peridiniales, Dinophyceae). Plankton Benthos Research 1, 183–190.

Kawami, M., van Wezel, R., Koeman, R.P.T., Matsuoka, K., 2009. *Protoperidinium tricingulatum* sp. nov. (Dinophyceae), a new motile form of a round brown, and spiny dinoflagellate cyst. Phycological Research 57, 259–267.

Kawamura, H., 2004. Dinoflagellate cyst distribution along a shelf to slope transect of an oligotrophic tropical sea (Sunda Shelf, South China Sea). Phycological Research 52, 355–375.

Kofoid, C.A., 1907. Dinoflagellates of the San Diego Region. III. Description of new species. University of California Publications in Zoology 3, 299–340.

Kofoid, C.A., Swezy, O., 1921. The free-living unarmored Dinoflagellata. Memoirs of the University of California 5, 1–538.

Kojima, N., 1989. 884. Dinoflagellate cyst analysis of Holocene sediment from Lake Hamana in central Japan. Transactions and Proceedings of the Palaeontological Society of Japan, New Series 155, 197–211.

Konieczny, R., 1983. En miljørettet palynologisk analyse av dinoflagellat-cyster i resente marine sedimenter fra Skagerak. Cand. Scient-oppgave i geologi, Universitetet I Oslo 1983. Unpublished MSc Thesis.

Krepakevich, A., Pospelova, V., 2010. Tracing the influence of sewage discharge on coastal bays of Southern Vancouver Island (BC, Canada) using sedimentary records of phytoplankton. Continental Shelf Research 30, 1924–1940.

Lankester, E.R., 1885. Protozoa. In: The Encyclopedia Britannica, 9th Edition, 19, 830–866.

Lebour, M.V., 1922. Plymouth Peridinians. I. *Diplopsalis lenticula* and its relatives. Journal of the Marine Biological Association of the United Kingdom 12, 795–812.

Lentin, J.K., Williams, G.L., 1976. A monograph of fossil peridinioid dinoflagellate cysts. Bedford Institute of Oceanography, Report Series, no. BI-R-75-16, 237 p. [Cover date 1975, issue date 1976]

Lentin, J.K., Williams, G.L., 1993. Fossil dinoflagellates: index to genera and species. 1993 edition. American Association of Stratigraphic Palynologists, Contributions Series 28, 856 + viii pp.

Lewis, J., 1990. The cyst-theca relationship of *Oblea rotunda* (Diplopsalidaceae, Dinophyceae). European Journal of Phycology 25, 339–351.

Lewis, J., Dodge, J.D., Tett, P., 1984. Cyst-theca relationships in some *Protoperidinium* species (Peridiniales) from Scottish sea lochs. Journal of Micropalaeontology 3, 25–34.

Li, Z., Han, M.-S., Matsuoka, K., Kim, S-Y., Shin, H.H., 2015a. Identification of the resting cysts of *Cochlodinium polykrikoides* Margalef (Gymnodiniales, Dinophyceae) in Korean coastal sediments. Journal of Phycology 51, 206–210.

Li, Z., Matsuoka, K., Shin, H.H., Kobayashi, S., Shin, K., Lee, T., Myung-Soo, H., 2015b. *Brigantedinium majusculum* is the cyst of *Protoperidinium sinuosum* (Protoperidiniaceae, Dinophyceae). Phycologia 54, 517–529.

Li., Z., Pospelova, V., Liu, L., Zhou, R., Song. B., 2017. High-resolution palynological record of Holocene climatic and oceanographic changes in the northern South China Sea. Palaeogeography, Palaeoclimatology, Palaeoecology 483, 94–124.

Limoges, A., Kielt, J.F., Radi, T., Ruiz-Fernandez, A.C., de Vernal, A., 2010. Dinoflagellate cyst distribution in surface sediments along the south-western Mexican coast (14.76 degrees N to 24.75 degrees N). Marine Micropaleontology 76, 104–123.

Liu, T., Mertens, K.N. Gu, H., 2015a. Cyst-theca relationship and phylogenetic positions of the diplopsaloideans (Peridiniales, Dinophyceae), with description of *Niea* and *Qia* gen. nov. Phycologia 54, 210–232.

Liu, T., Mertens, K.N., Ribeiro, S., Ellegaard, M., Matsuoka, K., Gu, H., 2015b. Cyst-theca relationships and phylogenetic positions of Peridiniales (Dinophyceae) with two anterior intercalary plates, with description of *Archaeperidinium bailongense* sp. nov. and *Protoperidinium fuzhouense* sp. nov. Phycological Research 63, 134–151.

Loeblich, A.R. Jr., Loeblich, A.R. III, 1966. Index to the genera, subgenera, and sections of the Pyrrhophyta. Studies in Tropical Oceanography 3, x+94 p.

Louwye, S, Head, M.J., De Schepper, S., 2004. Dinoflagellate cyst stratigraphy and palaeoecology of the Pliocene in northern Belgium, southern North Sea Basin. Geological Magazine 141, 353–378.

Margalef, R., 1961. Hidrografía y fitoplancton de un área marina de la costa meridional de Puerto Rico. Investigaciones Pesqueras 18, 33–96.

Matsuoka, K., 1985. Organic-walled dinoflagellate cysts from surface sediments of Nagasaki Bay and Senzaki Bay, west Japan. Faculty of Liberal Arts, Nagasaki University, Natural Science, Bulletin 25(2), 21–115.

Matsuoka, K., 1987. Organic-walled dinoflagellate cysts from surface sediments of Akkeshi Bay and Lake Saroma, North Japan. Bulletin of the Faculty of Liberal Arts, Nagasaki University (Natural Science) 28, 35–123.

Matsuoka, K., 1988. Cyst-theca relationship in the diplopsalid group (Peridiniales, Dinophyceae). Review of Palaeobotany and Palynology 56, 95−122.

Matsuoka, K., Fukuyo, Y., 1986. Cyst and motile morphology of a colonial dinoflagellate *Pheopolykrikos hartmannii* (Zimmermann) comb. nov. Journal of Plankton Research 8, 811−818.

Matsuoka, K., Fukuyo, Y., 1994. Geographical distribution of the toxic dinoflagellate *Gymnodinium catenatum* Graham in Japanese coastal waters. Botanica Marina 37, 495–504.

Matsuoka, K., Head, M.J., 2013. Clarifying cyst–motile stage relationships in dinoflagellates. In: Lewis, J. M., Marret, F., and Bradley, L. (eds), *Biological and Geological Perspectives of Dinoflagellates*. The Micropalaeontological Society, Special Publications. Geological Society, London, p. 325–350.

Matsuoka, K., Kawami, H., Fujii, R., H., Iwataki, M., 2006. Further examination of the cyst-theca relationship of *Protoperidinium thulesense* (Peridiniales, Dinophyceae) and the phylogenetic significance of round brown cysts. Phycologia 45, 632–641.

McMinn, A., 1993. 8. Neogene dinoflagellate cyst biostratigraphy from sites 815 and 823, Leg 133, Northeastern Australian margin. In: McKenzie, J.A., Davies, P.J., Palmer-Julson, A. et al. (eds.). Proceedings of the Ocean Drilling Program, Scientific Results 133, 97–105.

McMinn, A, Bolch, C.J.S., De Salas, M.F., Hallegraeff, G.M., 2010. Recent dinoflagellate cysts. In: Hallegraeff, G.M., Bolch, C.J.S., Hill, D.R.A., Jameson, I., LeRoi, J.M., McMinn, A., Murray, S., de Salas, M.F., Saunders, K. (eds.), Algae of Australia: Phytoplankton of Temperate Coastal Waters, Australian Biological Resources Study/CSIRO Publishing, pp. 260–292.

Mertens, K.N., González, C., Delusina, I., Louwye, S. 2009. 30 000 years of productivity and salinity variations in the late Quaternary Cariaco Basin revealed by dinoflagellate cysts. Boreas 38, 647–662.

Mertens, K.N., Rengefors, K., Moestrup, Ø., Ellegaard, M., 2012a. A review of recent freshwater dinoflagellate cysts: taxonomy, phylogeny, ecology and palaeocology. Phycologia 51, 612–619.

Mertens, K.N., Yamaguchi, A., Kawami, H., Ribeiro, S., Leander, B.S., Price, A.M., Pospelova, V., Ellegaard, M., Matsuoka, K., 2012b. *Archaeperidinium saanichi* sp nov.: a new species based on morphological variation of cyst and theca within the *Archaeperidinium minutum* Jorgensen 1912 species complex. Marine Micropaleontology 96–97, 48–62.

Mertens, K.N., Yamaguchi, A., Takano, Y., Pospelova, V., Head, M.J., Radi, T., Pieńkowski, A.J., de Vernal, A., Kawami, H., Matsuoka, K., 2013. A new heterotrophic dinoflagellate from the northeastern Pacific, *Protoperidinium fukuyoi*: Cyst–theca relationship, phylogeny, distribution and ecology. Journal of Eukaryotic Microbiology 60, 545–563.

Mertens, K.N., Takano, Y., Gu. H., Yamaguchi, A., Pospelova, V., Ellegaard. M., Matsuoka, K., 2015. The cyst-theca relationship of a new dinoflagellate with a spiny round brown cyst, *Protoperidinium lewisiae*, and its comparison to the cyst of *Oblea acanthocysta*. Phycological Research 63, 110–124.

Mertens, K.N., Gu, H., Takano, Y., Price, A.M., Pospelova, V., Bogus, K., Versteegh, G.J.M., Marret, F., Turner, R.E., Rabalais, N.N., Matsuoka, K., 2017. The cyst-theca relation of *Trinovantedinium pallidifulvum*, with erection of *Protoperidinium lousianensis* sp. nov. and their phylogenetic position within the *Conica* group. Palynology 41, 183–202.

Meunier, A., 1910. Microplancton des mers de Barents & de Kara. In: Duc d'Orléans Campagne Arctique de 1907. Bulens, Bruxelles, 355 pp.

Morquecho, L., Lechuga-Devéze, C.H., 2004. Seasonal occurrence of planktonic dinoflagellates and cyst production in relationship to environmental variables in subtropical Bahía Concepción, Gulf of California. Botanica Marina 47, 313–322.

Mudie, P.J., Marret, F., Mertens, K.N., Shumilovskikh, L., Leroy, S.A.G., 2017. Atlas of modern dinoflagellate cyst distributions in the Black Sea Corridor, including Caspian and Aral seas. Marine Micropaleontology 134, 1–152.

Narale, D.D., Patil, J.S., Anil, A.C., 2013. Dinoflagellate cyst distribution in recent sediments along the south-east coast of India. Oceanologia 55, 979–1003.

Nehring, S., 1994. Spatial distribution of dinoflagellate resting cysts in Recent sediments of Kiel Bight, Germany (Baltic Sea). Ophelia 39, 137–158.

Nie, D. 1943. Dinoflagellata of the Hainan region VI. On the genus *Diplopsalis*. Sinensia 14, 1–21.

Ostenfeld, C.H., 1902. Phytoplankton fra det Kaspiske Hav. (Phytoplankton from the Caspian Sea). Videnskabelige meddelelser fra den Naturhistoriske forening i Kjobenhavn 901, 129–139.

Palamarczuk, S., Barreda, V.D., 2000. Late Paleogene-Early Neogene palynology, Aries x-1 well, Argentina continental shelf, Tierrs del Fuego, Argentina. [Palinologia del Paleogeno tardio-Neogeno temprana, pozo Aries x-1, platforma continental Argentina, Tierra del Fuego.] Ameghiniana 37, 221–234

Pascher A. 1914. Über Flagellaten und Algen. Ber. Deutsche Botanische Gesellschaft, Berichte 32, 136–160.

Paulsen, O., 1905. On some Peridiniae and plankton diatoms. Meddelelser fra Kommissionen for Havundersøgelser, Serie Plankton 1(3), 1–7.

Paulsen, O., 1907. The Peridiniales of the Danish waters. Meddelelser fra Kommissionen for Havundersøgelser, Serie Plankton 1(5), 1–126.

Paulsen, O., 1931. Etudes sur le Microplancton de la mer d'Alboran. Instituto Español de oceanografía, Trabjos 4.

Pavillard, J., 1913. Le genre *Diplopsalis* Bergh et les genres voisins. Published by the author, Montpellier, France, 12 pp.

Pospelova, V., Head, M.J., 2002. *Islandinium brevispinosum* sp. nov. (Dinoflagellata), a new organic-walled dinoflagellate cyst from modern estuarine sediments of New England (USA). Journal of Phycology, 38, 593−601.

Pospelova, V., Kim, S.J., 2010. Dinoflagellate cysts in recent estuarine sediments from aquaculture sites of southern South Korea. Marine Micropaleontology 76, 37–51.

Pospelova, V., Chmura, G.L., Walker, H.A., 2004. Environmental factors influencing spatial distribution of dinoflagellate cyst assemblages in shallow lagoons of southern New England (USA). Review of Paleobotany and Palynology 128, 7–34.

Pospelova, V., Chmura, G.L., Boothman, W., Latimer, J.S., 2005. Spatial distribution of modern dinoflagellate cysts in polluted estuarine sediments from Buzzards Bay (Massachusetts, USA) embayments. Marine Ecology Progress Series 292, 23–40.

Pospelova, V., Esenkulova, S., Johannessen, S.C., O'Brien, M.C., Macdonald, R.W., 2010. Organic-walled dinoflagellate cyst production, composition and flux from 1996 to 1998 in the central Strait of Georgia (BC, Canada): a sediment trap study. Marine Micropaleontology 75, 17–37.

Pospelova, V., Pedersen, T.F., de Vernal, A., 2006. Dinoflagellate cysts as indicators of climatic and oceanographic changes during the past 40 kyr in the Santa Barbara Basin, southern California. Paleoceanography 21, 1−16, PA2010, doi:10.1029/2005PA001251, 2006.

Pospelova, V., Price, A., Pedersen, T.F., 2015. Palynological evidence for late Quaternary climate and marine primary productivity changes along the California margin. Paleoceanography 30(7), 877–894. doi: 10.1002/2014PA002728.

Potvin, É., Kim, S.-Y., Yang, E.J., Head, M.J., Kim, H.-C., Nam, S.-I., Yim, J.H., Kang, S.-H., 2018. *Islandinium minutum* subsp. *barbatum* subsp. nov. (Dinoflagellata), a new organic-walled dinoflagellate cyst from the western Arctic: morphology, phylogenetic position based on SSU rDNA and LSU rDNA, and distribution. Journal of Eukaryotic Microbiology 65, 750–772.

Prasad, V., Garg, R., Singh, V., Thakur, B., 2007. Organic matter distribution pattern in Arabian Sea: Palynofacies analysis from the surface sediments off Karwar coast (west coast of India). Indian Journal of Marine Science 36, 399–406.

Price, A., Pospelova, V. 2011. High-resolution sediment trap study of organic-walled dinoflagellate cyst production and biogenic silica flux in Saanich Inlet (BC, Canada). Marine Micropaleontology 80, 18–43.

Price, A.M., Mertens, K.N., Pospelova, V., Pedersen, T.F., Ganeshram, R.S., 2013. Late Quaternary climatic and oceanographic changes in the Northeast Pacific as recorded by dinoflagellate cysts from Guaymas Basin, Gulf of California (Mexico). Paleoceanography 28, 1–13.

Price, A., Pospelova, V., Coffin, M.R.S, Latimer, J.S., Chmura, G.L., 2016. Biogeography of dinoflagellate cysts in northwest Atlantic estuaries. Ecology and Evolution 6, 5648–5662.

Qi, Y.Z., Hong, Y., Zheng, L., Kulis, D.M., Anderson, D.M., 1996. Dinoflagellate cysts from Recent marine sediments of the south and east China Seas. Asian Marine Biology 13, 87–103.

Qiu, D., Huang, L., Liu, S., Zhang, H., Lin, S., 2013. Apical groove type and molecular phylogeny suggests reclassification of *Cochlodinium geminatum* as *Polykrikos geminatum*. PLoS ONE 8(8): e71346. doi:10.1371/journal.pone.0071346.

Reid, P.C., 1977. Peridiniacean and glenodiniacean dinoflagellate cysts from the British Isles. Nova Hedwigia 29, 429–463. [Volume dated 1978, preprint dated 18.11.1977]

Ribeiro, S., Lundholm, N., Amorim, A., Ellegaard, M., 2010. *Protoperidinium minutum* (Dinophyceae) from Portugal: cyst-theca relationship and phylogenetic position on the basis of single-cell SSU and LSU rDNA sequencing. Phycologia 49, 48–63.

Ribeiro, S., Amorim, A., Andersen, T.J., Abrantes, F., Ellegaard, M., 2012a. Reconstructing the history of an invasion: the toxic phytoplankton species *Gymnodinium catenatum* in the Northeast Atlantic. Biological Invasions 14, 969–985.

Ribeiro, S., Moros, M., Ellegaard, M., Kuijpers, A., 2012b. Climate variability in West Greenland during the past 1500 years: evidence from a high-resolution marine palynological record from Disko Bay. Boreas 41, 68–83.

Rochon, A., de Vernal, A., Turon, J.-L., Matthiessen, J., Head, M.J., 1999. Distribution of recent dinoflagellate cysts in surface sediments from the North Atlantic Ocean and adjacent seas in relation to sea-surface parameters. AASP Foundation Contributions Series 35, 1–152.

Sampedro, N., Fraga, S., Penna, A., Casabianca, S., Zapata, M., Grünewald, C.F., Riobó, P., Camp, J., 2011. *Barrufeta bravensis* gen. nov. sp. (Dinophyceae): a new bloom-forming species from the northwestern Mediterranean Sea. Journal of Phycology 47, 375–392.

Sarai, C., Yamaguchi, A., Kawami, H., Matsuoka, K., 2013. Two new species formally attributed to *Protoperidinium oblongum* (Aurivillius) Park et Dodge (Peridiniales, Dinophyceae): Evidence from cyst incubation experiments. Review of Palaeobotany and Palynology 192, 103–118.

Schiller, J., 1935. Dinoflagellatae (Peridineae) in monographischer Behandlung. 2. Teil, Lieferung 1. In: Kolkwitz, R., Zehnter Band. Flagellatae. In: Dr. L. Rabenhorst's Kryptogamen-Flora von Deutschland, Österreich und der Schweiz. Akademische Verlagsgesellschaft, Leipzig, Germany, 160 pp.

Schütt, F., 1895. Die Peridineen der Plankton-Expedition. Ergebnisse der Plankton-Expedition der Humboldt-Stiftung 4, 1–170, 27 pls.

Schütt, F., 1896. Peridiniales (Peridineae, Dinoflagellata, Cilioflagellata, arthrodele Flagellaten). In: Engler, A. and Prantl, K. (editors), Die natürlichen Pflanzenfamilien nebst ihren Gattungen und wichtigeren Arten insbesondere den Nutzpflanzen unter Mitwirkung zahlreicher hervorragender Fachgelehrten, Teil. 1, Abteilung 1b. Leipzig, Wilhelm Engelmann, p. 1–30.

Shin, H., Yoon, Y., Matsuoka, K., 2007. Modern dinoflagellate cysts distribution off the eastern part of Geoje Island, Korea. Ocean Science Journal 42, 31–39.

Shin, H.H., Matsuoka, K., Yoon, Y.H., Kim, Y.O., 2010a. Response of dinoflagellate cyst assemblages to salinity changes in Yeoja Bay, Korea. Marine Micropaleontology 77, 15–24.

Shin, H.H., Mizushima, K., Oh, S.J., Park, J.S., Noh, I.H., Iwataki, M., Matsuoka, K., Yoon, Y.H., 2010b. Reconstruction of historical nutrient levels in Korean and Japanese coastal areas based on dinoflagellate cyst assemblages. Marine Pollution Bulletin 60, 1243–1258.

Sonneman, J.A., Hill, D.R.A., 1997. A taxonomic survey of cyst-producing dinoflagellates from recent sediments of Victorian coastal waters, Australia. Botanica Marina 40, 149–177.

Sournia, A. 1973. Catalogue des espèces et taxons infraspécifiques de Dinoflagellés marins actuels. I. Dinoflagelles libres. Beihefte Nova Hedwigia 48, 1–92.

Sournia, A., 1984. Classification et nomenclature de divers dinoflagellés marins (Dinophyceae). Phycologia, 23, 345–355.

Sournia, A., 1986. Atlas du Phytoplancton Marin. Volume I: Introduction, Cyanophycées, Dictyochophycées, Dinophycées et Raphidophycées. Paris, Éditions du Centre National de la Recherche Scientifique, 216 p.

Stein, F.R. von, 1878. Der Organismus der Infusionsthiere nach eigenen Forschungen in systematischer Reihenfolge bearbeitet. III. Abteilung. Die Naturgeschichte der Flagellaten oder Geisselinfusorien. I. Hälfte. Den noch nicht abgeschlossenen allgemeinen Teil nebst Erklärung der sämmtlichen Abbildungen enthaltend. x+154 p., 24 pl.; Wilhelm Engelmann, Leipzig, Germany.

Stein, F.R. von, 1883. Der Organismus der Infusionsthiere nach eigenen Forschungen in systematischer Reihenfolge bearbeitet. II. Hälfte. Einleitung und Erklärung der Abbildungen. 30 p., 25 pl.; Wilhelm Engelmann, Leipzig, Germany.

Su-Myat, Maung-Saw-Htoo-Thaw, Matsuoka, K., Kin-Ko-Lay, Koike, K., 2012. Phytoplankton surveys off the southern Myanmar coast of the Andaman Sea: an emphasis on dinoflagellates including potentially harmful species. Fisheries Science 78, 1091–1106.

Tang, Y.Z., Gobler, C.J., 2012. The toxic dinoflagellate *Cochlodinium polykrikoides* (Dinophyceae) produces resting cysts. Harmful Algae 20, 71–80.

Taylor, F.J.R., 1976. Dinoflagellates from the International Indian Ocean Expedition. Biblioteca Botanica 132, 1–234, pl. 1–46.

Uddandam, P.R., Prasad, V., Biswajeet, T., Manoj, M.C., 2018. *Cristadinium striataserratum*: a dinoflagellate cyst from the Tropical region. Journal of the Palaeontological Society of India 53, 73−80.

Verleye, T.J., Mertens, K.N., Louwye, S., Arz, H.W., 2009. Holocene salinity changes in the southwestern Black Sea: A reconstruction based on dinoflagellate cysts. Palynology 33, 77–100.

Verleye, T., Pospelova, V., Mertens, K.N., Louwye, S., 2011. The geographical distribution and (palaeo)ecology of *Selenopemphix undulata* sp. nov., a new late Quaternary dinoflagellate cyst from the Pacific Ocean. *Marine Micropaleontology* 78, 65–83.

Wall, D., 1965. Modern hystrichospheres and dinoflagellate cysts from the Woods Hole region. Grana Palynologica 6, 297–316.

Wall, D., 1986. Dinoflagellate cysts and acritarchs from California current surface sediment. Unpublished PhD thesis, University of Saskatchewan, 305 pp.

Wall, D., Dale, B., 1968. Modern dinoflagellate cysts and evolution of the Peridiniales. Micropaleontology 14, 265−304.

Wall, D., Dale, B., Harada, K., 1973. Description of new fossil dinoflagellates from the Late Quaternary of the Black Sea. Micropaleontology 21, 18–31.

Williams, G.L, Bujak, J., 1977. Cenozoic palynostratigraphy of offshore eastern Canada. American Association of Stratigraphic Palynologists, Contributions Series 5A, 14–47.

Yamaguchi, A., Hoppenrath, M., Pospelova, V., Horiguchi, T., Leander, B.S., 2011. Molecular phylogeny of the marine sand-dwelling dinoflagellate *Herdmania litoralis* and an emended description of the closely related planktonic genus *Archaeperidinium* Jörgensen. European Journal of Phycology 46, 98–112.

Zevenboom, D., 1996. Late Oligocene–early Miocene dinoflagellate cysts from the Lemme-Carrosio section (NW Italy); biostratigraphy and palaeoenvironmental interpretation. Giornale di Geologia 3, 58/1−2, 81−93.

Zimmerman, W., 1930. Neue und wenig bekannte Kleinalgen von Neapel, I-V. Zeitschrift für Botanik, 23, 419−442.

Zingone, A., Montresor, M., 1988. *Protoperidinium parthenopes* sp. nov. (Dinophyceae), an intriguing dinoflagellate from the Gulf of Naples. Cryptogamie, Algologie 9, 117–125.

Zonneveld, K.A.F., 1996. Palaeoclimatic and palaeo-ecologic changes in the Eastern Mediterranean and Arabian Sea regions during the last deglaciation: a palynological approach to land-sea correlation. LPP Contributions Series, 3. Ponsen and Looijen, Wageningen, 200 pp.

Zonneveld, K.A.F., 1997. New species of organic-walled dinoflagellate cysts from modern sediments of the Arabian Sea (Indian Ocean). Review of Palaeobotany and Palynology 97, 319−337.

Zonneveld, K.A.F., Pospelova, V., 2015. A determination key for modern dinoflagellate cysts. Palynology 38, 387−409.

Zonneveld, K.A.F., Dale, B., 1994. The cyst-motile stage relationships of *Protoperidinium monospinum* (Paulsen) Zonneveld et Dale comb. nov. and *Gonyaulax verior* (Dinophyta, Dinophyceae) from the Oslo Fjord (Norway). Phycologia 33, 359–68.

Zonneveld, K.A.F., Ganssen, G., Troelstra, S., Versteegh, G.J.M., Visscher, H., 1997. Mechanisms forcing abrupt fluctuations of the Indian Ocean summer monsoon during the last deglaciation. Quaternary Science Reviews 16, 187−201.

Zonneveld, K.A.F., Marret, F., Versteegh, G.J.M., Bonnet, S., Bouimetarhan, I., Crouch, E., de Vernal, A., Elshanawany, R., Edwards, L., Esper, O., Forke, S., Grøsfjeld, K., Henry, M., Holzwarth, U., Kielt, J-F., Kim, S.Y., Ladouceur, S., Ledu, D., Chen, L., Limoges, A., Londeix, L., Lu, S.H., Mahmoud, M.S., Marino, G., Matsouka [sic], K., Matthiessen, J., Mildenhal [sic], D.C., Mudie, P., Neil, H.L., Pospelova, V., Qi, Y., Radi, T., Richerol, T., Rochon, A., Sangiorgi, F., Solignac, S., Turon, J.L., Verleye, T., Wang, Y., Wang, Z., Young, M., 2013. Atlas of modern dinoflagellate cyst distribution based on 2405 datapoints. Review of Palaeobotany and Palynology 191, 1–197.

Highlights

- 73 rare and endemic marine dinoflagellate cyst species are reviewed, described and illustrated.
- 9 belong to Gymnodiniales and 64 to Peridiniales.
- *Echinidinium aculeatum* and *Echinidinium transparantum* are validated.

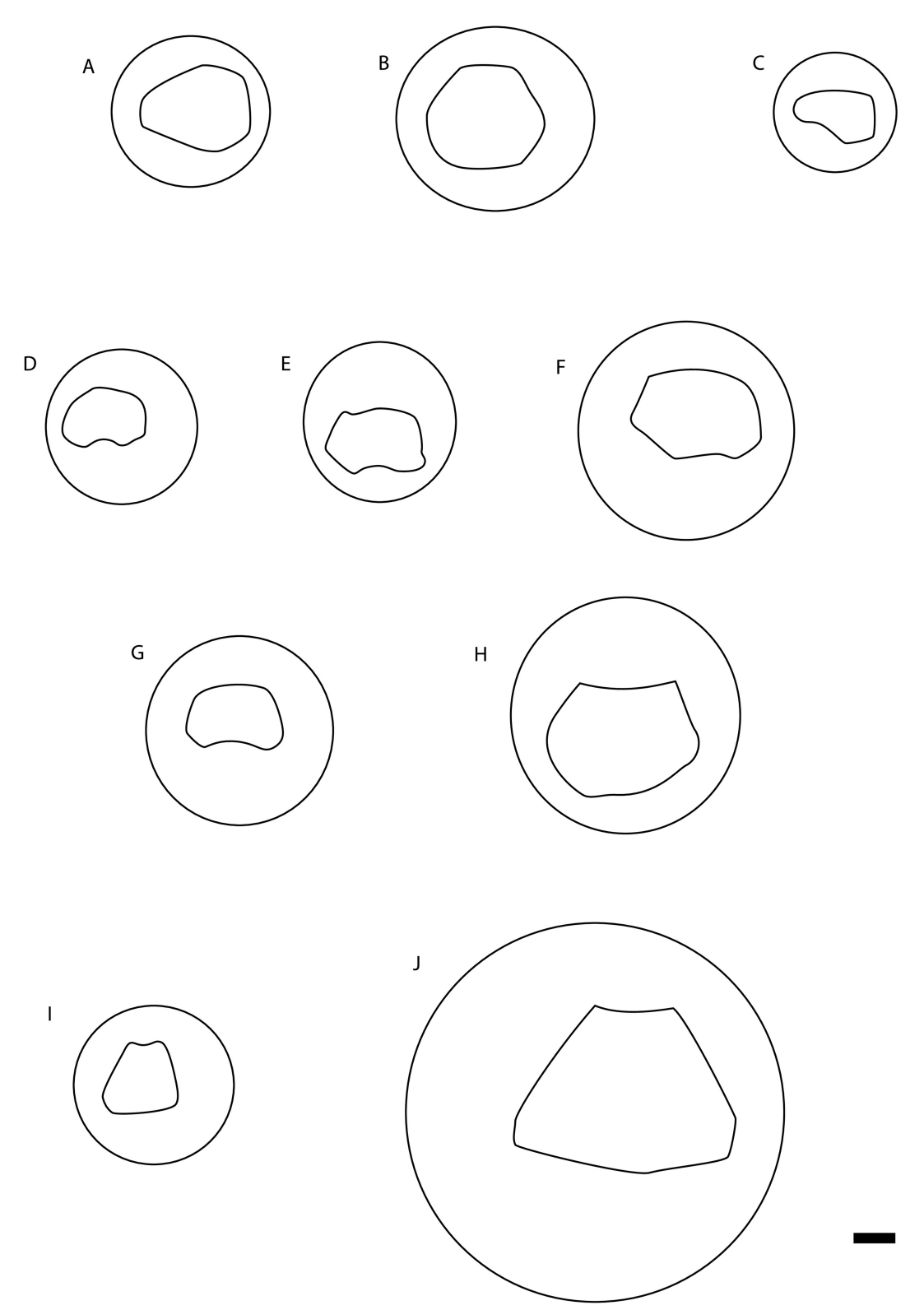

Figure 1

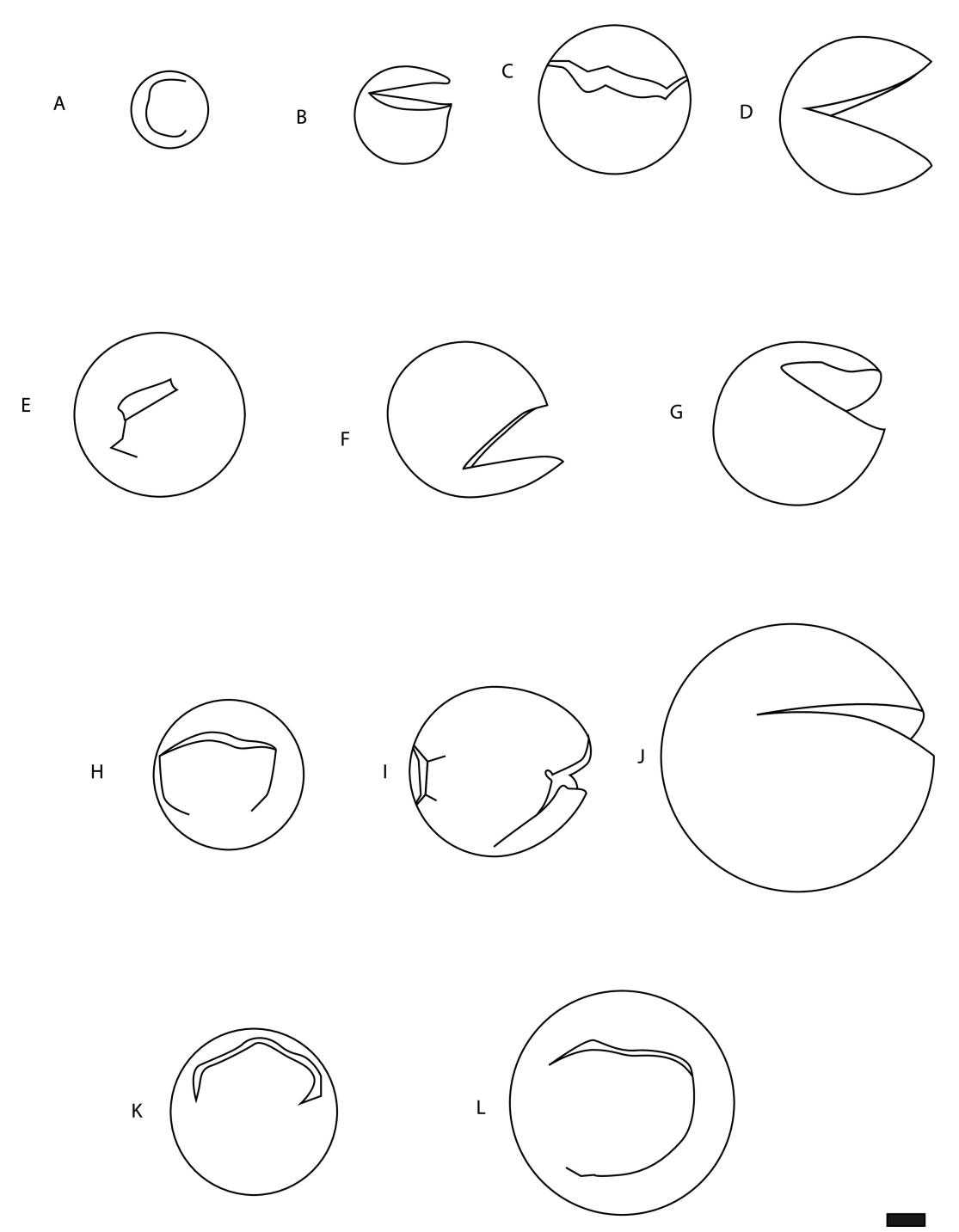

Figure 2